

**INVESTIGATION OF STRUCTURE AND PERMEABILITY OF  
SURFACES MODIFIED WITH SELF-ASSEMBLED MONOLAYERS**

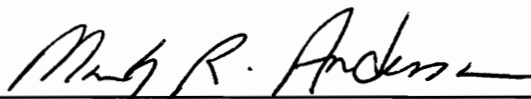
*by*

**Minhui Zhang**

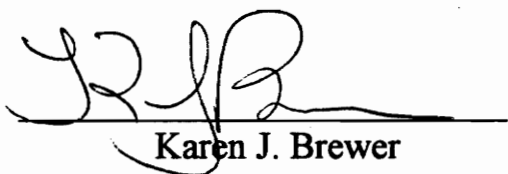
*Thesis submitted to the Faculty of the  
Virginia Polytechnic Institute and State University  
in partial fulfillment of the requirements for the degree of*

**Master of Science  
in  
Chemistry**

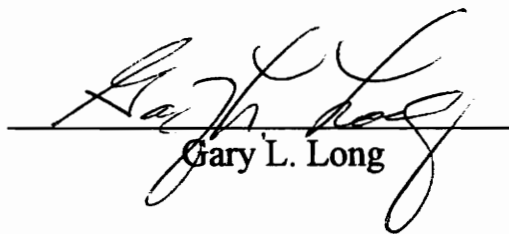
APPROVED:



Mark R. Anderson, Chairman



Karen J. Brewer



Gary L. Long

September, 1996  
Blacksburg, Virginia

**Keywords:** Monolayer, Thiol, Permeability, Dialkyl, Modified

LD  
5655  
V855  
1996  
Z435  
C.2

# INVESTIGATION OF STRUCTURE AND PERMEABILITY OF SURFACES MODIFIED WITH SELF-ASSEMBLED MONOLAYERS

by  
Minhui Zhang

Chairman: Dr. M. R. Anderson  
Department of Chemistry

(ABSTRACT)

This research focuses on how the structure of modified interfaces influence the behavior of the interface. Two groups of dialkyl sulfides are prepared and studied: a purely hydrocarbon dialkyl sulfide with the structure  $\text{CH}_3(\text{CH}_2)_{17}\text{S}(\text{CH}_2)_n\text{CH}_3$ , where  $n=7, 9, \text{ and } 17$ , and a carboxylic acid containing dialkyl sulfide with the structure  $\text{CH}_3(\text{CH}_2)_{17}\text{S}(\text{CH}_2)_m\text{COOH}$ , where  $m=7, 10, \text{ and } 15$ . The structure and the permeability of these monolayers are characterized by *ex situ* and *in situ* FTIR, contact angle measurements, and electrochemistry. It is found that the two groups of dialkyl sulfides have different surface structures and different monolayer-solution interfacial behaviors. The presence of a polar group, such as  $-\text{COOH}$ , within the monolayer structure is found to increase the charge transfer properties of the modified electrode by influencing the interfacial structure.

The structure and permeability of monolayers prepared from 15-mercaptopentadecanoic acid, 16-mercaptohexadecanoic acid, and their corresponding ethyl esters are also studied. Infrared spectroscopy and electrochemical permeability measurements indicate that the ester monolayers are ordered and have few differences in their structural and physical properties. Monolayers prepared from 15-mercaptopentadecanoic acid and 16-mercaptohexadecanoic acid, however, are structurally and physically different from the esters and each other. The IR and contact angle results indicate that hydrogen bonding interactions between the terminal groups of the monolayers influence the structural organization and physical properties of the monolayer. The extent of the hydrogen bonding interactions within the  $\omega$ -mercaptoalkanoic acid monolayers appear to be related to the structure of the interface, suggesting that the orientation of the terminal functional group influences its ability to interact within the monolayer.

## **Acknowledgments**

I thank my advisor, Mark R. Anderson, for his kind and insightful direction to my graduate research. He is not only my research advisor, but also a good personal friend to me. I thank my committee members for their academic suggestions and help to my research project: Dr. Karen Brewer, and Dr. Gary Long.

I thank many research groups in chemistry department for allowing me to use their equipment and chemicals: McNair group, Kingston group, Gibson group, Taylor group, and Long group.

Many thanks to my fellow students at Virginia Tech for their camaraderie. Just list a few of them: Howard Ding, Xiaowei Sun, Ziqi Sun, Edwin Lancaster, Ronna Cadorette, Ron Earp, Jimin Huang, Reed Edwards, Yuwen Wang, and Hong Zhuang.

Finally, I am especially grateful for the understanding, patience, support, and love of my family: my parents, my wife, my sister, and my five-year old little son. This degree is for them.

## Table of Contents

|  |      |
|--|------|
| Abstract.....  | ii   |
| Acknowledgments .....  | iv   |
| List of Figures.....   | vi   |
| List of Tables .....   | viii |
| Chapter 1 Introduction and Literature Review.....  | 1    |
| 1.1 Research Objectives.....   | 1    |
| 1.2 Literature Review.....   | 1    |
| 1.3 Introduction: Characterization of Self-Assembled<br>Monolayers (SAM) .....                           | 9    |
| Chapter 2 Experimental .....   | 15   |
| 2.1 Chemicals Preparation .....  | 15   |
| 2.2 Monolayer Preparation .....  | 16   |
| 2.3 Electrochemical Measurement.....   | 16   |
| 2.4 Contact Angle Measurement .....  | 18   |
| 2.5 Infrared Spectroscopy .....  | 18   |
| Chapter 3 Charge Transfer Properties of Monolayers Prepared from<br>Unsymmetrical Dialkyl Sulfides ..... | 21   |
| 3.1 Infrared Spectroscopy .....  | 21   |
| 3.1.1 Ex situ IRRAS of Hydrocarbon Dialkyl Sulfide<br>Monolayers .....                                   | 21   |
| 3.1.2 Ex situ IRRAS of Acid Containing Dialkyl Sulfide<br>Monolayers .....                               | 24   |
| 3.1.3 In situ PM-FTIRRAS of Dialkyl Sulfide<br>Monolayers .....  | 27   |
| 3.2 Wettability.....   | 27   |
| 3.2.1 Contact Angle Measurements with water .....  | 27   |
| 3.2.2 Contact Angle titrations.....  | 31   |

|  |    |
|--|----|
| 3.2.3 Contact Angle Measurements with hexadecane ..  | 33 |
| 3.3 Electrochemical Measurements .....   | 34 |
| 3.3.1 Charging Current Measurements .....  | 34 |
| 3.3.2 Cyclic Voltammetry .....   | 38 |
| Chapter 4 Investigation of Terminal Functional Group Effects on<br>Monolayers Prepared from w-Mercaptoalkanoic Acids ..... | 44 |
| 4.1 Infrared Spectroscopy .....  | 45 |
| 4.1.1 Comparison of IR Spectra in C-H region.....  | 45 |
| 4.1.2 Comparison of Carbonyl Stretch in IR Spectra ...   | 49 |
| 4.2 Contact Angle Measurements.....  | 53 |
| 4.3 Electrochemistry: Charging Current Measurements.....   | 54 |
| 4.4 Discussion and Conclusion.....   | 57 |
| Chapter 5 Summary .....  | 60 |
| References.....  | 62 |
| Vita.....  | 65 |

## List of Figures

|   |    |
|---|----|
| Figure 1.1. Diagram of alkanthiol monolayer adsorbed on gold surface. ....  | 11 |
| Figure 2.1. Drop cell for electrochemical measurements. ....  | 17 |
| Figure 2.2. Optical layout of PM-FTIRRAS. ....  | 19 |
| Figure 3.1. Reflection infrared spectra of the carbon-hydrogen region for the monolayers prepared from the hydrocarbon dialkyl sulfides .   | 22 |
| Figure 3.2. Reflection infrared spectra for the monolayers prepared from the acid containing dialkyl sulfides. ....   | 25 |
| Figure 3.3. Comparison of the <i>ex situ</i> and <i>in situ</i> infrared spectra for $\text{CH}_3(\text{CH}_2)_{17}\text{S}(\text{CH}_2)_{15}\text{COOH}$ . ....                                  | 28 |
| Figure 3.4. Plot of the measured contact angle versus pH of the sessile drop prepared from phosphate buffering species. ....  | 32 |
| Figure 3.5. Cyclic voltammetry data in the presence of the hydrocarbon dialkyl sulfide modified electrodes for aqueous 0.10 M NaCl solutions. ....  | 35 |
| Figure 3.6. Cyclic voltammetry data in the presence of the acid containing dialkyl sulfide modified electrodes for aqueous 0.10 M NaCl solutions. ....  | 37 |
| Figure 3.7. Cyclic voltammetry data for the oxidation of 0.004 M $\text{Fe}(\text{CN})_6^{4-}$ in the presence of aqueous 0.10 M KCl at the hydrocarbon dialkyl sulfide modified electrodes. .... | 41 |
| Figure 3.8. Voltammetry data for the oxidation of 0.004M $\text{Fe}(\text{CN})_6^{4-}$ in the presence of aqueous 0.10 M KCl at the acid containing dialkyl sulfide modified electrodes. ....     | 42 |



|   |    |
|---|----|
| Figure 4.1. Reflection Infrared spectra of the C-H region for monolayers prepared from $\omega$ -substituted acids and corresponding ethyl esters .....                       | 46 |
| Figure 4.2. Reflection Infrared spectra of the low energy region of the spectrum for monolayers prepared from $\omega$ -substituted ethyl esters....                          | 50 |
| Figure 4.3. Reflection Infrared spectra of the low energy region of the spectrum for monolayers prepared from $\omega$ -substituted acids .....                               | 51 |
| Figure 4.4. Current vs. Potential response to 0.10 M aqueous KCl at 100mV/sec for gold electrodes modified with tetradecanethiol and $\omega$ -substituted ethyl esters ..... | 55 |
| Figure 4.5. Current vs. Potential response to 0.10 M aqueous KCl at 100mV/sec for gold electrodes modified with $\omega$ -substituted acids.....                              | 56 |

## List of Tables

|  |    |
|--|----|
| Table 1.1. Mode assignments for alkanethiol monolayers on gold surface . . . . .   | 13 |
| Table 3.1. Peak Positions for the Carbon-Hydrogen Region of the Infrared Spectra for the Unsymmetrical Dialkyl Sulfide Monolayers.   | 23 |
| Table 3.2. Peak Position for the Carbon-Hydrogen Region of the <i>in situ</i> Spectra of the Unsymmetrical Dialkyl Sulfide Monolayers.....                                   | 29 |
| Table 3.3. Advancing Contact Angle Measured by the Sessile Drop Method for the Dialkyl Sulfide Modified Surfaces with Water and Hexadecane.....                              | 30 |
| Table 3.4. Thickness of the Unsymmetrical Dialkyl Sulfide Monolayers Measured by Optical Ellipsometry. ....  | 39 |
| Table 4.1. Peak position and peak width data for the reflection infrared spectra of monolayers prepared from $\omega$ -substituted acids and corresponding ethyl esters..... | 47 |

# Chapter 1

## Introduction and Literature Review

### 1.1 Research Objectives

The objective of this research project was to develop a better understanding of how the structure of organic monolayers adsorbed on gold surfaces influence the physical properties of the interface. The characterization of the monolayer structure and properties was by infrared spectroscopy, contact angle measurement, and electrochemistry. The study focused on the role of polar functional groups (-COOH in our case) within the monolayer in determining the ordering of the monolayer, and how these functional groups influenced interaction between the monolayer and the adjacent environment.

### 1.2 Literature Review

The Langmuir-Blodgett (LB) technique is a method commonly used to generate organic monolayers/multilayers on solid surfaces [1]. In this technique, surfactant is spread over an aqueous solution, and then a solid support is dipped into the solution and the organic film is deposited onto the solid surface. Scientists are interested in LB films because they are promising structures for investigations of the microscopic origins of complex interfacial properties such as wetting (contact angle behavior), adhesion, interfacial reactivity, electron-transfer kinetics, and molecular adsorption. Despite this interest, the difficulty in preparing LB films has limited the popularity of this method in scientific research.

In 1983, Nuzzo and Allara identified a new way to more easily modify metallic interfaces [1]. They demonstrated that a strong chemical bond was formed between *Au* surfaces and the sulfur atom of organic mercaptans, resulting in an organized organic monolayer on the gold surface, provided that the carbon chain is sufficiently long (more than 10 carbons). Upon characterization by external reflection FTIR, ellipsometry, and XPS (X-ray Photoelectron Spectroscopy), it was found that the alkyl chains were in all trans configuration, with the interface having crystalline-like properties. The alkyl chains were found to tilt about  $30^\circ$  relative to the surface normal within these monolayers.

Since the adsorption of organic mercaptans has proven to be a convenient method of surface modification, a tremendous amount of research work has been done in this area [2]. Electrochemists are active in this area because these modified interfaces provide an ideal model to study fundamental issues such as electron-transfer events at the electrochemical interface. Although a wealth of research has been conducted since the pioneering work of Nuzzo and Allara, the understanding of the structural and physical properties of self-assembled monolayers still needs to improve. Some important aspects, such as surface disorder and terminal group interactions within monolayers, need to be further clarified. For example, it is well known that introducing a terminal functional group into the monolayer structure may cause surface disorder and charge transport enhancement [12], but the underlying mechanism of how the structural and physical properties are affected is not clear. It is not clear from the data which factors cause the change of charge transport properties of the

monolayer, the disorder itself or the functionality within the monolayer. On the other hand, some terminal functional group (such as -COOH) tend to interact with other. It is also necessary to find out the influence of functional group interactions upon the structural and physical properties of the monolayers. Thus, our research project is intended to be a comprehensive study of these important issues.

Since 1983, a large variety of monolayers prepared from different mercaptan compounds have been analyzed. They can be roughly categorized as the following types: (1) Pure alkane thiol compounds. These compounds have long carbon chains ( $> 10$  carbons) and can form largely defect-free, crystalline-like monolayers on gold substrates. (2)  $\omega$ -substituted thiol compounds. These compounds can be represented as a general formula  $\text{HS}(\text{CH}_2)_n\text{X}$ , where  $X$  may be a wide range of functional groups. So far many types of  $\omega$ -substituted have been synthesized and analyzed, including: (a)  $X =$  alkyl ether [3]; (b)  $X =$  carboxylic acid [4]; (c)  $X =$  hydroxy; (d)  $X =$  electroactive group [5], such as ferrocene; (e)  $X =$  polyethylene glycol [6]; (f)  $X =$  group with large dipole, such as  $\text{SO}_2$  group [7]. (3) Binary systems.  $\omega$ -substituted thiol compounds coadsorbed with pure alkane thiol compounds have been utilized to show how the physical properties of the modified surface are affected by the terminal functional groups [11, 12]. (4) Dialkyl sulfides. Troughton *et al.* have shown that dialkyl sulfides can be adsorbed onto gold surface spontaneously, resulting in reasonably stable monolayer structures. These dialkyl sulfides could be utilized to control the structure/composition of the monolayer [8].

In the first part of our research project, pure hydrocarbon and acid containing dialkyl sulfides were synthesized and analyzed. In the second part of the research project,  $\omega$ -substituted thiol compounds were used.

Although the regular nature of self-assembled monolayers has been investigated by many research groups because of their theoretical potential (for example, as a model of membrane structure) and their promise for practical applications (for example, wetting, lubrication, adhesion, and charge transfer), their usage has been problematic for other researchers. The reason is that self-assembled monolayers form well defined, crystalline-like structure, which is impenetrable to aqueous solutions. The charge transfer properties of the monolayer modified surfaces is, therefore, decreased by the impenetrability of the aqueous solution. Intentionally-formed defect monolayer structures are sometimes desired, especially for electrochemical applications.

Sagiv was the first to report the intentional perforation of self-assembling monolayers of alkylsiloxanes on the substrates [9]. He showed that such membranes could effectively readsorb molecules of approximately the same size and shape as the molecules used to induce the perforations. Rubinstein *et al.* used a mixed monolayer of octadecyltrichlorosilane and octadecanethiol molecules as a barrier restricting access of redox species in solution to the electrode surface [11]. Crooks *et al.* [12] coadsorbed an *n*-alkanethiol with 4-HTP (4-hydroxythiophenol) or *p*-thiocresol forming a nanoporous monolayer structure. The *n*-alkanethiol molecules act as an inert electron- and mass-transfer-blocking layer; while the functionalized, aromatic organomercaptan molecules act as electron-transfer sites. The

number of defect sites on the surface is found to be a function of the relative concentrations of the two mercaptans in the bulk deposition solution. They demonstrated that it is possible to use binary mercaptan solutions to prepare functionally composite monolayers. The chemical nature of the template /framework, and the template/framework ratio of the deposition solution control the size, number, and chemical characteristics of the defects.

These research efforts indicate that functional groups within the monolayer can behave like a gate or channel to allow aqueous solution to penetrate through. How these functional groups function to determinate the physical properties of the monolayer surface is not clear. Apparently, the monolayers in these methods are disordered, but the relationship between the disorder itself and the existence of a functional group is not addressed.

Another interesting issue is the positioning of the functional groups in the monolayer structure. Chidsey [5] have shown a scheme in which ferrocene centers were spaced away from the electrode surface by a fixed distance corresponding to the thickness of the hydrocarbon layer of the self-assembled molecules. This system served to investigate long-range electron-transfer kinetics of the ferrocene centers. Because the distance is controllable, it allowed a study of the details the distance dependence of electron transfer rates. They found that longer chain lengths and lower ferrocene surface concentrations result in slower electron-transfer kinetics with the ferrocene groups. This result reveals that the positioning of the functional group in the monolayer structure is also important in determining the physical properties of the monolayer. In our research project, different chain length of carboxylic acid dialkyl sulfides were synthesized in the hope

of characterizing the positional influence in determining the charge transport properties of monolayer structure.

In addition to introducing a surface defect to enhance charge transport properties of the monolayer structure, another approach to increase charge transport is attributed to the compatibility of the organic-nature monolayer with either the organic solvent or the organic solute. Finklea *et al.* presented an important paper which demonstrated facile electron transfer at an octadecanethiol modified gold electrode [13]. They found that oxidation of ferrocene in acetonitrile solutions on the modified electrode had significant faradaic current, while the same modified electrode completely prevented the oxidation of ferrocyanide in aqueous solutions [13]. They interpreted this result as the ability of the acetonitrile solvent to solvate the organic monolayer. On the other hand, aqueous solution is unable to solvate the organic monolayer, resulting the poor electron transfer properties. Similar results were presented by Groat and Creager [39]. They found that an equilibrium existed between the monolayer modified surface and the organic media due to the ability of the organic solvent to solvate the organic species adsorbed on surface. For the same reason, using neutral organic solutes instead of charged solutes also exhibited better electron transfer properties [14, 15].

The influence of organic solvents on the structure of the organic monolayer is further emphasized by *in situ* spectroscopic results. Sandroff *et al.* used surface enhanced Raman spectroscopy to study the structure of a hexadecanethiol monolayer in the presence of aqueous solutions and chloroform solutions [16]. These results suggested that the outer portions



of the monolayer was solvated by the chloroform. Similar results were presented by Porter *et al.* [17] and Anderson *et al.* [18] using *in situ* infrared spectroscopy to study the octadecanethiol monolayer structure. It was found that aqueous solutions had little impact on the monolayer structure, while some minor disruption of the surface structure was suggested when organic solvent was used.

It is well known that the presence of chemical functionality within the monolayer can influence the structure and properties of the interface. This influence is thought to be caused by the strong terminal group interactions and/or steric effects. But it is not clear which is the more dominant reason for the influence. Miller *et al.* studied  $\omega$ -hydroxyalkanethiol monolayers [19, 20]. They found that, due to the strong terminal group interactions with each other,  $\omega$ -hydroxyalkanethiol can form monolayers with greater order than the analogous methyl terminated monolayers. In other words, they believe that the terminal group interactions are a dominant effect in this case. On the contrary, by investigating a series of monolayers prepared from  $\omega$ -substituted thiol compounds, Chidsey and Loiacono found that the monolayer permeability and disorder was influenced by the degree of steric and electrostatic interaction between the functionality of the interface [21].

A comprehensive study regarding the function of the terminal groups within the monolayer structure is necessary. In the second part of our research project, two groups of thiol compounds were used to investigate this issue. One group of the thiol compounds,  $\omega$ -mercaptoalkanoic acids, were used to represent strong terminal group interactions, while their corresponding ethyl esters, were used to represent steric effects. By

comparing the monolayers prepared from these two groups of compounds, the importance of the terminal group interactions and/or steric effects should be revealed.

Some research groups noticed another interesting fact that only a single methylene group difference in monolayer chains may cause significant differences in structures and properties of monolayer interfaces. This so-called "even-odd" effect even exists in methyl terminated monolayers. It was found that the tilt of the alkyl chain, as well as the even or odd number of methylene groups in the alkyl chain determined the projection of the methyl group with regard to the surface normal [22, 23]. Consequently, interfacial properties such as permeability and surface wettability were greatly affected by the projection of the methyl group. Although the "even-odd" effect is an important observation, its importance compared with other factors which also influence the monolayer structure is not clear. More importantly, if the projection of the terminal functional groups is influenced by an even-odd effect, the tendency for the terminal functional groups to interact with each other is consequently influenced. It is not clear either from previous research how important such an influence is. In the second part of the project, two  $\omega$ -mercaptoalkanoic acids were prepared with only one methylene group difference between each other, in the hope that the projection of terminal groups and the tendency to form intermolecular interactions could be studied.

It is clear that the surface structure of monolayers and its interfacial properties are complicated phenomena, determined by many different factors. These factors include monolayer disorder, solvent compatibility of

the monolayer, the existence and positioning functional group within the monolayer, interactions among the functional groups, even-odd effect, etc. Each factor has its own contribution to the structural and physical properties of the monolayer. More importantly, these factors are entwined with each other and influence with each other. Clearly, the studies of the monolayers by simply isolating one of the factors may lead to a biased interpretation of the measured data. Therefore, a comprehensive investigation of these factors by using a more sophisticated monolayer system is necessary to improve our knowledge of interfacial properties of self-assembled monolayers. With these considerations in mind, we used two groups of dialkyl sulfides and two groups of  $\omega$ -substituted thiol compounds in the research project.

### **1.3 Introduction: Characterization of Self-Assembled Monolayers (SAM)**

SAM interfaces can be prepared by submerging a clean metal surface (gold, silver, etc.) into a dilute solution of the compound which can form monolayer. It is an easier procedure than the Langmuir-Blodgett technique for preparation of modified interfaces. Thiol compounds with long alkyl chains are probably the most popular species to form monolayers on gold substrates. The adsorption process is due to the strong chemical bond formed between the *Au* atom and the sulfur atom [24].

In order to form well defined monolayers on a gold surface, an alkyl chain with more than 10 methylene carbons is necessary. The driving force for the monolayer organization is maintained by Van der Waals forces between the methylene groups of the adjacent chains. When formed, the

carbon chain tilts approximately  $30^\circ$  with regard to surface normal (figure 1.1) [25].

Many experimental methods have been developed to characterize the SAM modified surfaces. Among these techniques, electrochemical measurement, contact angle measurement, and IR spectroscopy are the most frequently used.

Electrochemistry measurements provide information about the charge transport properties of SAM modified surfaces. It has been found that *n*-alkanethiol modified surface can completely block electron transport to species in aqueous solution [13, 21, 29]. Electrochemistry measurements show that by introducing defects into the monolayer, either through structural disorder or by solvent/solute compatibility, the electron transport properties of the surface can be enhanced.

Wettability is the ability of a liquid to spread over a surface. This property of surfaces is both theoretically and practically important. It has been shown that the wettability of a solid is determined by the structure of its outer most few angstroms [8, 28]. Contact angle measurement is a very sensitive technique to measure the wettability of a surface. It can give information about the microscopic chemical nature (hydrophobic or hydrophilic) and/or heterogeneity of the surface.

Infrared Reflection-Absorption Spectroscopy (IRRAS) can provide a large amount of structural information about the SAM surfaces. According to Allara *et al.* [22], there are two ways monolayer structures can be interpreted from FTIR spectra: (a) differences in line shapes and peak frequencies are usually indicative of differences in intra- and intermolecular

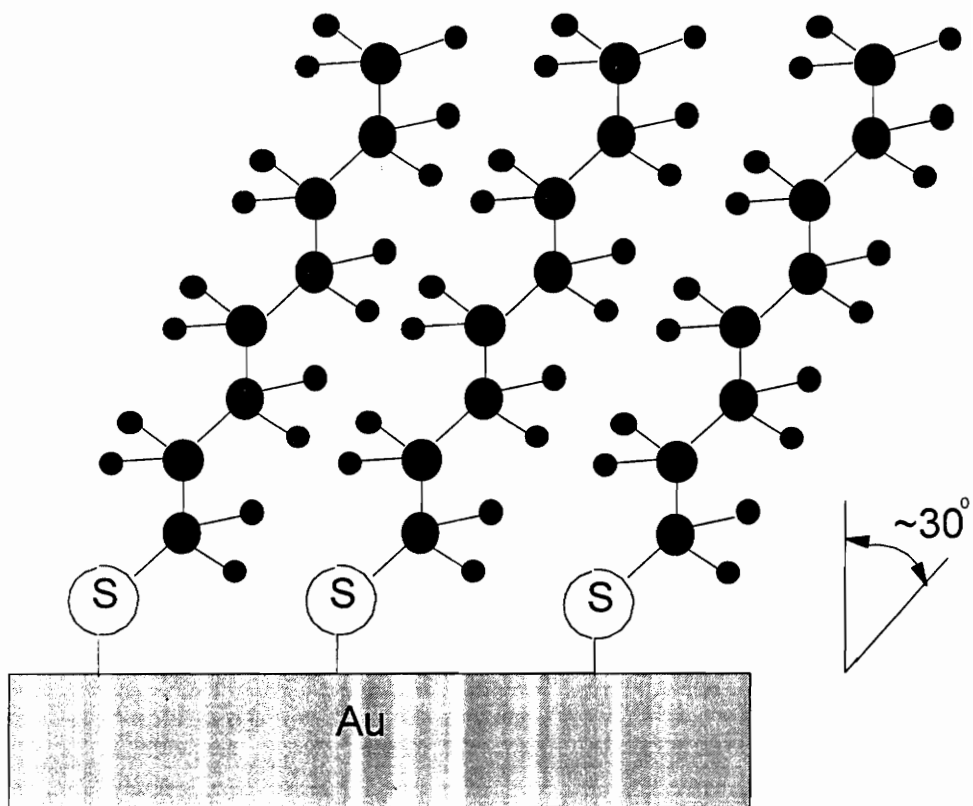


Figure 1.1. Diagram of alkanthiol monolayer adsorbed on gold surface. The size of atoms are not to scale.

packing; (b) intensity differences are usually indicative of monolayer coverage and structural anisotropy. By calculation and comparison with IR spectra of pure thiol compounds, the mode assignments for some typical IR peaks of *n*-alkanethiol monolayers are widely accepted [22, 26]. Table 1.1 summarizes the important IR peaks.

The IRRAS technique is based upon the "surface selection rule" [27]. IR radiation, like any light, is composed of a p-polarization component, in which the electric vector is parallel to the plane of propagation, and an s-polarization component, in which the electric vector is perpendicular to the plane of propagation. For s-polarized light, when the light is reflected by a metallic surface, the electric vector phase shifts by 180 degree. On the other hand, the p-polarized light will have nearly 90 degree phase shift when the light reflects at a grazing angle ( $\sim 79$  degree). As a consequence, the intensity of the p-polarized light will be enhanced at the reflection surface. The absorbance by a thin film deposited at a metal surface, therefore, can be detected only by p-polarized light when the incident radiation is at a grazing angle.

Based upon the same theory, *in situ* IR measurement of monolayers can be conducted by PM-IRRAS (Polarization Modulation IRRAS), a technique utilized to increase sensitivity for surface confined species. In this technique, monolayers on the surface absorb only the p-polarized light, while the bulk environment absorb both s- and p-polarized light. The detector signal is passed to a lock-in amplifier which detects the IR signal at the frequency of the polarization modulation. The output from lock-in

Table 1.1. Mode assignments for alkanethiol monolayers on gold surface [22].

| Frequency<br>cm <sup>-1</sup> | Mode Assignment                  | Features                                  |
|-------------------------------|----------------------------------|---|
| 2962                          | CH <sub>3</sub> C-H asym str, ip |   |
| 2955                          | CH <sub>3</sub> C-H asym str, op |   |
| 2943                          | CH <sub>3</sub> C-H sym str, FR  |   |
| 2918                          | CH <sub>2</sub> C-H asym str     | indicative of<br>crystalline-like packing |
| 2872                          | CH <sub>3</sub> C-H sym str, FR  |   |
| 2850                          | CH <sub>2</sub> C-H sym str      | indicative of<br>crystalline-like packing |
| 1471                          | CH <sub>2</sub> scissors def.    |   |
| 1372                          | CH <sub>3</sub> def.             |   |
| ~1150-<br>1350                | chain wags and twists            |   |

nomenclature: str = stretch, asym = antisymmetric, sym = symmetric  
 ip = in-plane, op = out-plane, FR = Fermi resonance,  
 def = deformation

amplifier is the intensity difference of s- and p-polarized light,  $I_s - I_p$ . The signal which bypassed the high pass filter and the lock-in amplifier consists of both s- and p-polarized light, equaling  $I_s + I_p$ . The ratio of  $I_s - I_p$  and  $I_s + I_p$  gives the spectral information of only the surface-bound species.

Since electrochemistry measurement, contact angle measurement, and IR measurement are the most important methods to characterize SAM modified surface, we used these methods in our research project.



## Chapter 2 Experimental

### 2.1 Chemicals Preparation

All chemicals, unless otherwise noted, were purchased from Aldrich Chemical Co. (Milwaukee, WI) and were used as received.

Three acid containing dialkyl sulfides were prepared using the procedure described by Troughton *et al.* [8]. Here, octadecanethiol was substituted by an appropriate n-bromoalkanoic acid in the presence of sodium metal and degassed methanol solvent. For the preparation of  $\text{CH}_3(\text{CH}_2)_{17}\text{S}(\text{CH}_2)_{15}\text{COOH}$ , the 16-bromohexadecanoic acid was first prepared by bromide substitution of the hydroxide of 16-hydroxyhexadecanoic acid using the method of Bain *et al.* [30]. The  $\omega$ -mercaptoalkanoic acids, which were also used in the second part of the research project, were prepared from the corresponding  $\omega$ -bromoalkanoic acid using the method of Bain *et al.* [30]. The purely hydrocarbon dialkyl sulfides were prepared by reaction of the appropriate 1-bromoalkane with octadecanethiol. Intermediates and final products were checked by NMR, IR, and melting point measurements.

The ethyl esters were prepared by esterification of the  $\omega$ -mercaptoalkanoic acids catalyzed by acid in ethanol solutions. Here, the appropriate  $\omega$ -mercaptoalkanoic acid was reacted with absolute ethanol solution in the presence of 100  $\mu\text{l}$  concentrated  $\text{H}_2\text{SO}_4$ . Monolayers prepared by this procedure had reflection infrared spectra identical to ester monolayers prepared by Nuzzo *et al.* [22].

## 2.2 Monolayer Preparation

The 1 in. × 1 in. gold substrates were purchased from Evaporated Metal Films, Inc. (Ithaca, NY). The surface-bound species were dissolved in chloroform or ethanol solution depending on the solubility. The concentration was controlled at 0.005 M. Monolayer preparation was conducted by immersing the cleaned gold substrates into the solution [18]. Prior to adsorption, the gold substrates were cleaned in "piranha" solution (25% peroxide - 75% sulfuric acid) for one minute. *Extreme caution should be exercised with piranha solutions because they are potentially explosive. Following usage, piranha solutions should be immediately disposed* [31]. The substrates were kept in the adsorption solution for 24 hours. When removed from the solution, the modified gold surfaces were rinsed with ethanol followed by distilled water and were then dried by blowing with a rapid stream of nitrogen.

## 2.3 Electrochemical Measurement

Electrochemical measurements were conducted using a "drop" electrochemical cell (figure 2.1). By adjusting the syringe properly, the cell establishes a drop contact with the monolayer modified surface with an effective working area of 0.066 cm<sup>2</sup>. The electrode potential was controlled by an EG&G Princeton Applied Research (Princeton, NJ) Model 273 potentiostat/galvanostat which was interfaced to an IBM Model 50Z microcomputer running EG&G Princeton Applied Research Model 270 electrochemical software. For the charging current measurements, cyclic voltammetry experiments were conducted with aqueous solutions

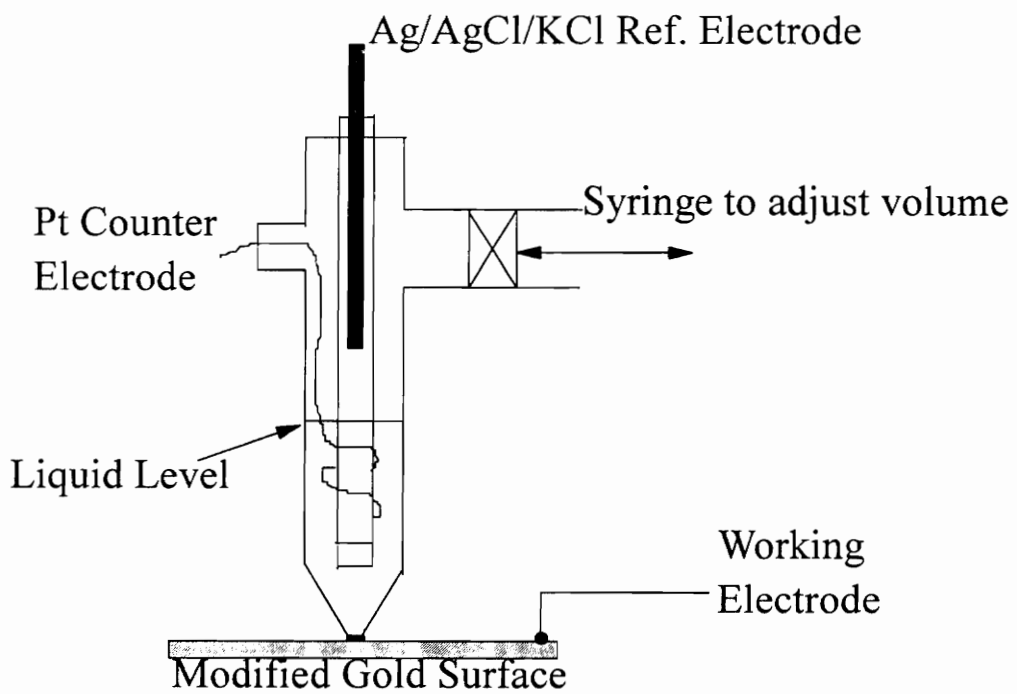


Figure 2.1. Drop cell for electrochemical measurements .

containing 0.10 M NaCl. Cyclic voltammetry experiments were conducted with aqueous 0.10 M KCl solutions containing 0.004M  $K_4Fe(CN)_6$ . The water used as a solvent in these electrochemical experiments was purified by a Barnsted Nanopure water purification system. The potential scan rate for all experiment was controlled at 0.10 V/s. The surface roughness factor was estimated to be 1.2 by the method of Porter *et al* [29].

## 2.4 Contact Angle Measurement

Contact angles were measured on a Rame-Hart, Inc., NRL contact angle goniometer. The size of the solvent drop was 5  $\mu$ l. At least 5 drops were measured for each surface. For the contact angle titrations, buffer solutions of various pH values were prepared using sodium phosphate species, maintaining constant ionic strength (0.20 M) for all buffers.

## 2.5 Infrared Spectroscopy

Infrared measurements were conducted with a Nicolet Model 710 FTIR (Madison, WI) spectrometer using a liquid nitrogen cooled HgCdTe detector. *Ex situ* spectra were collected at 2  $cm^{-1}$  resolution using a Spectra Tech (Stamford, CT) FT80 specular reflectance attachment. For each monolayer sample, at least three parallel measurements were conducted in order to ensure correct data collection. *In situ* infrared spectra were obtained with 4  $cm^{-1}$  resolution using the polarization modulation Fourier transform infrared reflection absorption spectroscopy (PM-FTIRRAS) method [18]. The optical layout of PM-FTIRRAS is shown as figure 2.2.  $D_2O$  used for the *in situ* spectroscopy of the monolayers was obtained from Cambridge Isotopes Laboratories (Woburn, MA). Spectral analysis and

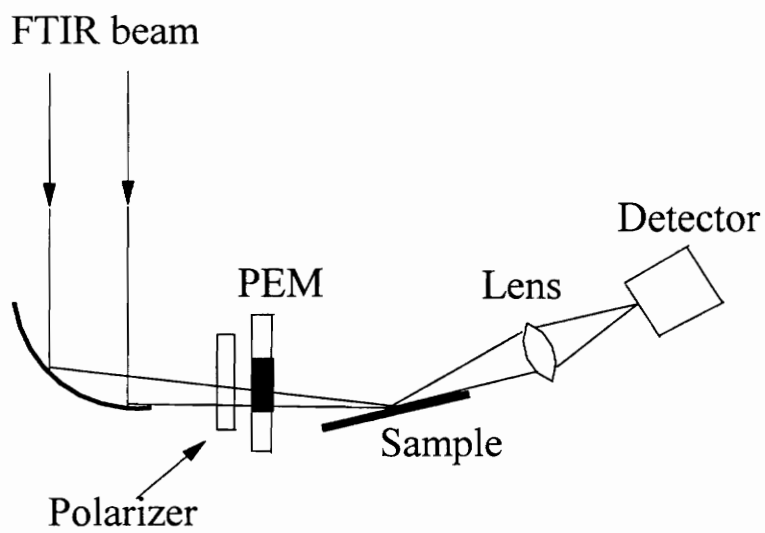


Figure 2.2. Optical layout of PM-FTIRAS.

peak fitting were conducted using Spectra Calc Software (Galactic Industries Corp., Salem, NH). For *in situ* experiments, at least three parallel measurements were conducted also.

## Chapter 3

### Charge Transfer Properties of Monolayers Prepared from Unsymmetrical Dialkyl Sulfides

The first part of this research focuses on the spontaneous adsorption of unsymmetrical dialkyl sulfides to study how two monolayer properties, structural disorder and solvent compatibility, influence interfacial charge transfer properties. Two groups of dialkyl sulfides are prepared and studied: a purely hydrocarbon dialkyl sulfide with the structure  $\text{CH}_3(\text{CH}_2)_{17}\text{S}(\text{CH}_2)_n\text{CH}_3$ , where  $n=7, 9,$  and  $17,$  and an acid containing dialkyl sulfide with the structure  $\text{CH}_3(\text{CH}_2)_{17}\text{S}(\text{CH}_2)_m\text{COOH}$ , where  $m=7, 10,$  and  $15.$  The structure and the permeability of these monolayers are characterized by *ex situ* and *in situ* FTIR, contact angle measurements, and electrochemistry.

### 3.1 Infrared Spectroscopy

#### 3.1.1 *Ex situ* IRRAS of Hydrocarbon Dialkyl Sulfide Monolayers

*Ex situ* IRRAS of purely hydrocarbon dialkyl sulfide monolayers are shown in figure 3.1. From the spectra, it is obvious that all three hydrocarbon dialkyl sulfides have similar asymmetric and symmetric methylene vibrations, in terms of their peak position and peak area. The methylene absorptions are found at approximately  $2926$  and  $2854 \text{ cm}^{-1}$  (table 3.1), respectively, for all of the monolayers. According to Allara *et al.*, these peak positions suggest that a fluid or disordered structure exists in the monolayer [29]. The asymmetric methyl vibrational mode is found at

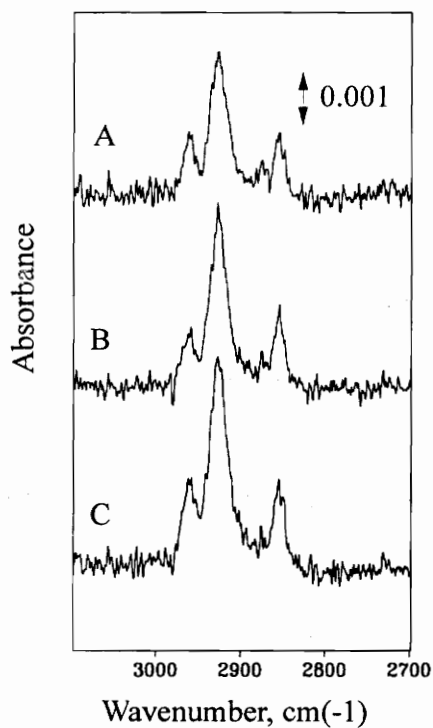


Figure 3.1. Reflection infrared spectra of the carbon-hydrogen region for the monolayers prepared from the hydrocarbon dialkyl sulfides. Spectrum A corresponds to  $\text{CH}_3(\text{CH}_2)_{17}\text{S}(\text{CH}_2)_{17}\text{CH}_3$ , B to  $\text{CH}_3(\text{CH}_2)_{17}\text{S}(\text{CH}_2)_9\text{CH}_3$ , and C to  $\text{CH}_3(\text{CH}_2)_{17}\text{S}(\text{CH}_2)_7\text{CH}_3$ .



Table 3.1. Peak Positions ( $\text{cm}^{-1}$ ) for the Carbon-Hydrogen Region of the Infrared Spectra for the Unsymmetrical Dialkyl Sulfide Monolayers.

| Compounds  | $\text{CH}_3$ , a | $\text{CH}_2$ , a       | $\text{CH}_2$ , s |
|--|-------------------|-------------------------|-------------------|
| $\text{CH}_3(\text{CH}_2)_{17}\text{S}(\text{CH}_2)_{17}\text{CH}_3$ | 2961              | 2926<br>(0.066)         | 2855<br>(0.025)   |
| $\text{CH}_3(\text{CH}_2)_{17}\text{S}(\text{CH}_2)_9\text{CH}_3$    | 2961              | 2925<br>(0.077)         | 2854<br>(0.021)   |
| $\text{CH}_3(\text{CH}_2)_{17}\text{S}(\text{CH}_2)_7\text{CH}_3$    | 2961              | 2926<br>(0.10)          | 2854<br>(0.016)   |
| $\text{CH}_3(\text{CH}_2)_{17}\text{S}(\text{CH}_2)_{15}\text{COOH}$ | 2962              | 2919,<br>2928<br>(0.12) | 2850<br>(0.026)   |
| $\text{CH}_3(\text{CH}_2)_{17}\text{S}(\text{CH}_2)_{10}\text{COOH}$ | 2963              | 2918,<br>2925<br>(0.12) | 2850<br>(0.034)   |
| $\text{CH}_3(\text{CH}_2)_{17}\text{S}(\text{CH}_2)_7\text{COOH}$    | 2963              | 2918,<br>2926<br>(0.16) | 2851<br>(0.036)   |

approximately  $2961\text{ cm}^{-1}$ , which is a slightly lower energy compared with the corresponding peak of octadecanethiol monolayers. If the monolayer structure was ordered, there should exist a symmetric methyl stretch split by Fermi resonance which is found at about  $2872\text{ cm}^{-1}$ . But from figure 3.1, the Fermi resonance mode is clearly absent, suggesting structural disorder within the monolayer [17, 32]. The disorder within the monolayer is not surprising, because it is obviously difficult for the dialkyl sulfides to try to align their alkyl chains within the monolayer [8]. Our *ex situ* spectra of pure hydrocarbon dialkyl sulfide monolayers are consistent with those by Troughton and co-workers for similar monolayers [8].

### 3.1.2 *Ex situ* IRRAS of Acid Containing Dialkyl Sulfide Monolayers

Figure 3.2 shows the spectra for the acid containing dialkyl sulfide monolayers, and the peaks are summarized in table 3.1. One significant observation is that the shape of the asymmetric methylene peaks is unsymmetrical in nature and with an apparent shoulder to higher energy. By deconvolution and peak fitting, it is found that this absorption was composed of two bands, one was at  $2918\text{ cm}^{-1}$  and another one at approximately  $2926\text{ cm}^{-1}$ . We ruled out the possibility that the asymmetry is caused by the symmetric methyl stretch which is split by Fermi resonance, because like the pure hydrocarbon dialkyl sulfide monolayers, the corresponding Fermi resonance feature at  $2875\text{ cm}^{-1}$  is also absent from the spectrum of the acid containing dialkyl sulfides. In addition, this spectral feature is at an energy lower than is typically observed for the symmetric methyl Fermi resonance mode. Based upon the above

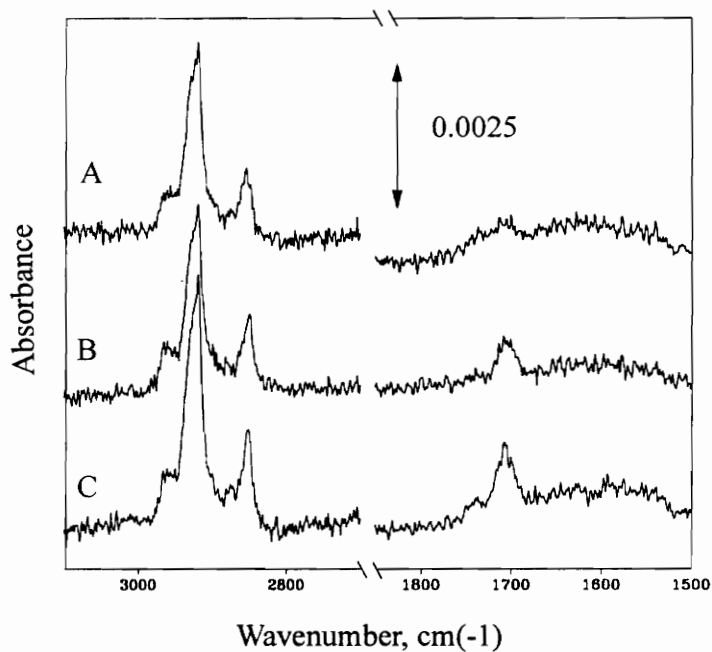


Figure 3.2. Reflection infrared spectra for the monolayers prepared from the acid containing dialkyl sulfides, showing both the carbon-hydrogen and the carbonyl regions of the spectra. Spectrum A corresponds to  $\text{CH}_3(\text{CH}_2)_{17}\text{S}(\text{CH}_2)_{15}\text{COOH}$ , B to  $\text{CH}_3(\text{CH}_2)_{17}\text{S}(\text{CH}_2)_{10}\text{COOH}$ , and C to  $\text{CH}_3(\text{CH}_2)_{17}\text{S}(\text{CH}_2)_7\text{COOH}$ .

observation and reasons, we believe that a mixed structure existing in the acid containing dialkyl sulfide monolayers, with a portion of the monolayer ordered (band at 2918  $\text{cm}^{-1}$ ), and another portion having a fluid-like structure (band at 2926  $\text{cm}^{-1}$ ). This is a similar structure with those described by Bain and Whitesides [33, 34]. The symmetric methylene mode is found at 2850  $\text{cm}^{-1}$ , which is also suggestive of an ordered monolayer.

Peaks found at about 1705  $\text{cm}^{-1}$  are attributed to carboxylic acid groups involved in hydrogen bonding interactions [35]. A small peak at 1736  $\text{cm}^{-1}$  is suggested in the spectrum, but it is barely distinguishable from the noise. According to other research reported in the literature, a peak at 1736  $\text{cm}^{-1}$  may be assigned to a carboxylic acid group which is not involved, or only weakly involved in hydrogen bonding interactions [22, 35]. Another interesting observation is that the intensity of the carbonyl absorption is related to the relative position of the acid group with regard to sulfur atom of the dialkyl sulfide. The intensity of the carbonyl decreases as the acid group is placed further from the sulfur atom, and nearly disappears for the monolayer prepared with  $\text{CH}_3(\text{CH}_2)_{17}\text{S}(\text{CH}_2)_{15}\text{COOH}$ . This observation suggests that an orientational effect takes place, namely, the carbonyl vibration becomes aligned parallel to the electrode surface as its position in the monolayer is changed [8]. We believe this observation is important and should have its significant impact on interfacial phenomenon, and this leads to our second part of research, which will be addressed in Chapter 4.

### 3.1.3 *In situ* PM-FTIRRAS of Dialkyl Sulfide Monolayers

The PM-FTIRRAS technique provides a convenient and direct way to study the interfacial structure of monolayers in contact with environmental media. Here, D<sub>2</sub>O solutions were used to investigate how these dialkyl sulfide monolayers respond to condensed media. For the pure hydrocarbon dialkyl sulfides, it is found that there were no significant changes in the peak positions of the asymmetric and symmetric methylene modes compared to *ex situ* spectrum (table 3.2). For the acid containing dialkyl sulfide monolayers, however, the observation is different (figure 3.3, and table 3.2). The asymmetric methylene mode at about 2918 cm<sup>-1</sup>, which is characteristic of ordered monolayer structure, disappears and a single band at approximately 2926 cm<sup>-1</sup> is observed. As we mentioned before, this peak position is typically associated with disordered, fluid-like monolayer structures. As for the symmetric methylene mode, the result is consistent with the asymmetric methylene mode: the peak shifts to higher energy (2853 cm<sup>-1</sup>) with the *in situ* spectra, suggesting a fluid monolayer structure. The *in situ* spectral results suggest that the aqueous solution has little effect upon the surface structure of the hydrocarbon dialkyl sulfides, while causing disordering of the acid containing dialkyl sulfide monolayers.

## 3.2 Wettability

### 3.2.1 Contact Angle Measurements with water

Contact angle measurements with water and hexadecane provide additional evidence of a disordered surface structure (table 3.3). The

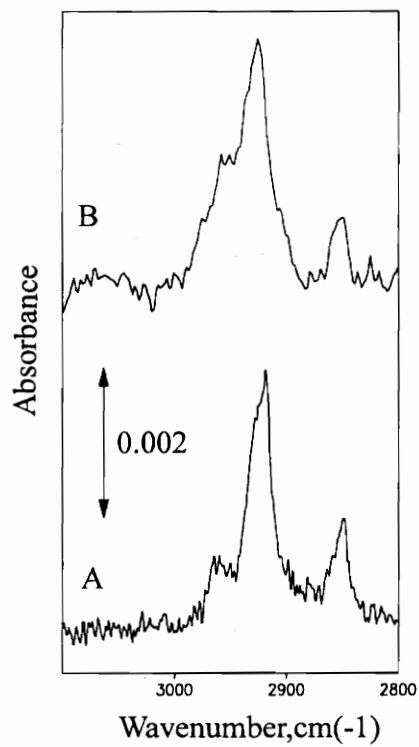


Figure 3.3. Comparison of the *ex situ* (A) and *in situ* (B), in the presence of D<sub>2</sub>O, infrared spectra for CH<sub>3</sub>(CH<sub>2</sub>)<sub>17</sub>S(CH<sub>2</sub>)<sub>15</sub>COOH.

Table 3.2. Peak Position ( $\text{cm}^{-1}$ ) for the Carbon-Hydrogen Region of the in situ Spectra of the Unsymmetrical Dialkyl Sulfide Monolayers

| Compound   | $\text{CH}_3, \text{a}$ | $\text{CH}_2, \text{a}$ | $\text{CH}_2, \text{s}$ |
|--|-------------------------|-------------------------|-------------------------|
| $\text{CH}_3(\text{CH}_2)_{17}\text{S}(\text{CH}_2)_{17}\text{CH}_3$ | $2959 \pm 4$            | $2926 \pm 2$            | $2852 \pm 1$            |
| $\text{CH}_3(\text{CH}_2)_{17}\text{S}(\text{CH}_2)_9\text{CH}_3$    | $2964 \pm 4$            | $2924 \pm 2$            | $2854 \pm 4$            |
| $\text{CH}_3(\text{CH}_2)_{17}\text{S}(\text{CH}_2)_7\text{CH}_3$    | $2956 \pm 4$            | $2926 \pm 3$            | $2855 \pm 4$            |
| $\text{CH}_3(\text{CH}_2)_{17}\text{S}(\text{CH}_2)_{15}\text{COOH}$ | $2956 \pm 4$            | $2925 \pm 4$            | $2854 \pm 4$            |
| $\text{CH}_3(\text{CH}_2)_{17}\text{S}(\text{CH}_2)_{10}\text{COOH}$ | $2955 \pm 4$            | $2925 \pm 2$            | $2851 \pm 2$            |
| $\text{CH}_3(\text{CH}_2)_{17}\text{S}(\text{CH}_2)_7\text{COOH}$    | $2958 \pm 4$            | $2924 \pm 3$            | $2855 \pm 2$            |

Table 3.3. Advancing Contact Angle Measured by the Sessile Drop Method for the Dialkyl Sulfide Modified Surfaces with Water and Hexadecane.

| Compound   | water      | hexadecane |
|--|------------|------------|
| $\text{CH}_3(\text{CH}_2)_{17}\text{S}(\text{CH}_2)_{17}\text{CH}_3$ | $99 \pm 1$ | $36 \pm 2$ |
| $\text{CH}_3(\text{CH}_2)_{17}\text{S}(\text{CH}_2)_9\text{CH}_3$    | $99 \pm 2$ | $19 \pm 1$ |
| $\text{CH}_3(\text{CH}_2)_{17}\text{S}(\text{CH}_2)_7\text{CH}_3$    | $95 \pm 1$ | $18 \pm 2$ |
| $\text{CH}_3(\text{CH}_2)_{17}\text{S}(\text{CH}_2)_{15}\text{COOH}$ | $93 \pm 1$ | $6 \pm 1$  |
| $\text{CH}_3(\text{CH}_2)_{17}\text{S}(\text{CH}_2)_{10}\text{COOH}$ | $95 \pm 3$ | $9 \pm 2$  |
| $\text{CH}_3(\text{CH}_2)_{17}\text{S}(\text{CH}_2)_7\text{COOH}$    | $99 \pm 2$ | $8 \pm 2$  |
| octadecanethiol  | $99 \pm 3$ | $45 \pm 1$ |



surface prepared from the hydrocarbon dialkyl sulfide monolayers had only slightly lower contact angle than was found for the octadecanethiol monolayer modified surface. The slightly lower values measured for the hydrocarbon dialkyl sulfides may be due to the disorder that is present within the dialkyl sulfide monolayers. For the acid containing dialkyl sulfide monolayers, it is found that contact angles of water were relatively high. A relationship is found to exist between the value of contact angle and the position of the polar acid group with regard to the surface. As the acid group is placed closer to the monolayer surface, the aqueous contact angle decreases slightly. This result indicates some influence of the polar acid group on the interfacial properties.

### **3.2.2 Contact Angle titrations**

Contact angle titrations with buffered aqueous solutions were used to further investigate the influence of the acid group upon the interfacial properties (figure 3.4). As a comparison, 11-mercaptoundecanoic acid modified surface were also subject to contact angle titration. The contact angle for an 11-mercaptoundecanoic acid modified surface has a clear transition when the pH value is changed from 6 to 8. This observation makes sense in terms of classical acid-base titrations. For the acid containing dialkyl sulfides, the experimental observations are not so simple. Unlike the 11-mercaptoundecanoic acid monolayer, none of the dialkyl sulfides has a clear transition when pH values pass through the expected  $pK_a$  for organic acids. Secondly, for the  $CH_3(CH_2)_{17}S(CH_2)_7COOH$

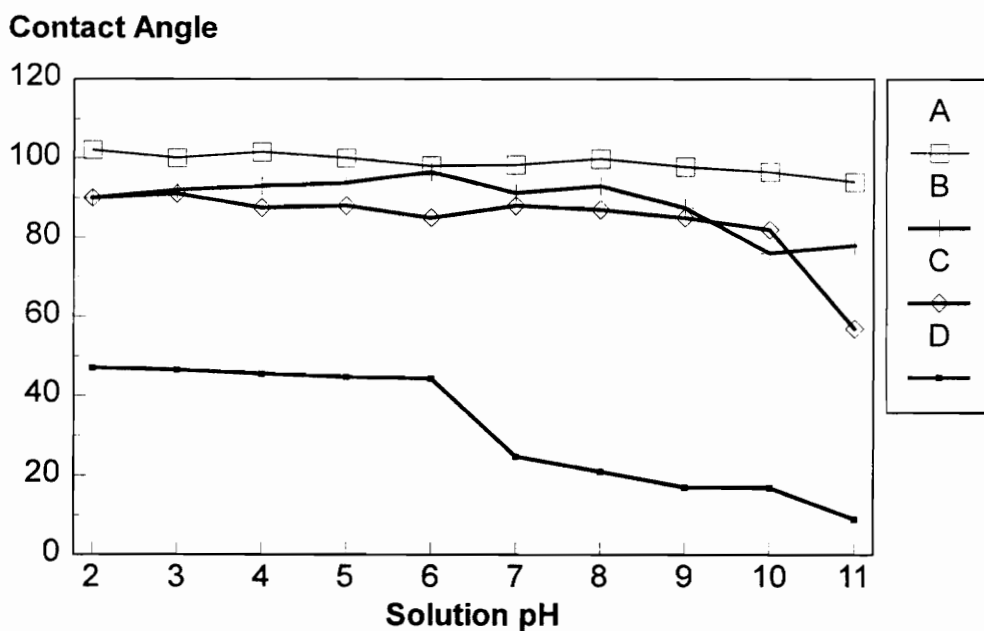


Figure 3.4. Plot of the measured contact angle versus pH of the sessile drop prepared from phosphate buffering species. A correspond to the data for the  $\text{CH}_3(\text{CH}_2)_{17}\text{S}(\text{CH}_2)_7\text{COOH}$  monolayer, B to the data for the  $\text{CH}_3(\text{CH}_2)_{17}\text{S}(\text{CH}_2)_{10}\text{COOH}$  monolayer, C to the data for the  $\text{CH}_3(\text{CH}_2)_{17}\text{S}(\text{CH}_2)_{15}\text{COOH}$  monolayer, and D to the data for a monolayer prepared from 11-mercaptoundecanoic acid.

monolayer, the contact angle does not vary much with the pH of the sessile drop. This indicates that the polar acid group is isolated from the buffer solution. In other words, the hydrophobic hydrocarbon methylene groups may protect the acid group from contacting the buffer solution directly. Finally, as was found in contact angle measurement of water, the positioning of the polar acid group with respect to the substrate is important. As the acid group is placed closer to the monolayer interface, the effect of pH upon the measured contact angle increases. As can be seen in figure 3.4, the contact angle decreases for both  $\text{CH}_3(\text{CH}_2)_{17}\text{S}(\text{CH}_2)_{10}\text{COOH}$  and  $\text{CH}_3(\text{CH}_2)_{17}\text{S}(\text{CH}_2)_{15}\text{COOH}$  when the pH is greater than approximately 8.5, with the effect being slightly larger for the  $\text{CH}_3(\text{CH}_2)_{17}\text{S}(\text{CH}_2)_{15}\text{COOH}$  monolayer. While the high pH has the effect of decreasing the contact angle, no clear transition is observed as it was with the 11-mercaptoundecanoic acid monolayer. This observation also is consistent with the previous conclusion that for all three of the dialkyl sulfide monolayers, the acid group is buried to a different extent under the methylene groups, and is unable to contact the outer solution completely. This conclusion is consistent with the finding of Troughton *et al.* [8].

### 3.2.3 Contact Angle Measurements with hexadecane

Contact angle measurements were also conducted with hexadecane (table 3.3). For the purely hydrocarbon dialkyl sulfide monolayers, the contact angles with hexadecane varied from  $19^\circ$  to  $36^\circ$ , significantly lower than that of the octadecanethiol monolayer surface ( $45^\circ$ ). This result is thought to indicate that the purely hydrocarbon dialkyl sulfide monolayers

have exposed methylene groups at the interface [34]. For the acid containing dialkyl sulfides, the contact angle made with hexadecane is approximately  $8^\circ$ , values even lower than those of the purely hydrocarbon dialkyl sulfides. We believe that such significantly low value of the contact angle indicates either (i) a significant amount of methylene groups exposed at the surface, and/or (ii) exposure of the acid groups at the interface. Since it is found that the acid group is somewhat protected by the methylene groups from the contact angle measurement with water, the hexadecane contact angle measurement suggests that (i) may be a better description of the monolayer structure.

### **3.3 Electrochemical Measurements**

#### **3.3.1 Charging Current Measurements**

Figure 3.5 shows the charging current for the purely hydrocarbon dialkyl sulfide modified electrodes to an aqueous 0.10M NaCl solution. As a comparison, the response of a octadecanethiol modified electrode is also shown. The striking feature is that the charging current responses are approximately the same for all three pure hydrocarbon dialkyl sulfide monolayers, and they have almost no difference with that measured for the octadecanethiol modified electrode. This observation suggests that despite the somewhat disordered surface structure of the pure hydrocarbon dialkyl sulfide surface, the permeability of aqueous solutions is still limited to the same range of an "ideally" packed surface (i.e. octadecanethiol modified electrode, in this case). In other words, the *in situ* dimensions of the three

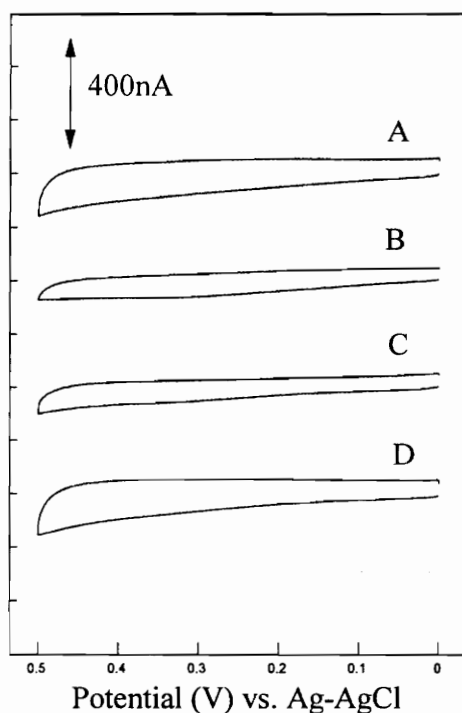


Figure 3.5. Cyclic voltammetry data in the presence of the hydrocarbon dialkyl sulfide modified electrodes for aqueous 0.10 M NaCl solutions. Voltammogram A corresponds to the data for the  $\text{CH}_3(\text{CH}_2)_{17}\text{S}(\text{CH}_2)_{17}\text{CH}_3$  monolayer, B to the data for the  $\text{CH}_3(\text{CH}_2)_{17}\text{S}(\text{CH}_2)_9\text{CH}_3$  monolayer, C to the data for  $\text{CH}_3(\text{CH}_2)_{17}\text{S}(\text{CH}_2)_7\text{CH}_3$ , and D to the data for an octadecanethiol monolayer for comparison. The voltammetric data were collected at a potential scan rate of 0.10 V/s with an electrode having a surface area of  $0.066 \text{ cm}^2$ .

pure hydrocarbon dialkyl sulfide surface are almost the same as each other and have no significant difference with that of octadecanethiol modified surface.

Figure 3.6 shows the charging current response for the acid containing dialkyl sulfide monolayers. The spectra are obviously different from figure 3.5. The charging current increases as the acid group is placed closer to the monolayer-solution interface. This indicates that greater permeation of aqueous solution happens when the acid group gets closer to the interface. We attribute this effect to the influence of the positioning of the acid group. Previous studies showed that polar carboxylic acid groups within the monolayer structure could influence interfacial interaction if the acid group is less than five methylene groups from the interface [8, 33, 36]. Our charging current data for the acid containing dialkyl sulfide monolayers suggests that the proximity of the acid group to the interface increases the ability of aqueous solvent to penetrate through the monolayer structure. For the  $\text{CH}_3(\text{CH}_2)_{17}\text{S}(\text{CH}_2)_7\text{COOH}$  monolayer, despite the somewhat disordered structure suggested by IR (*ex situ* and *in situ*) and contact angle measurements, the charging current is almost the same as that measured for

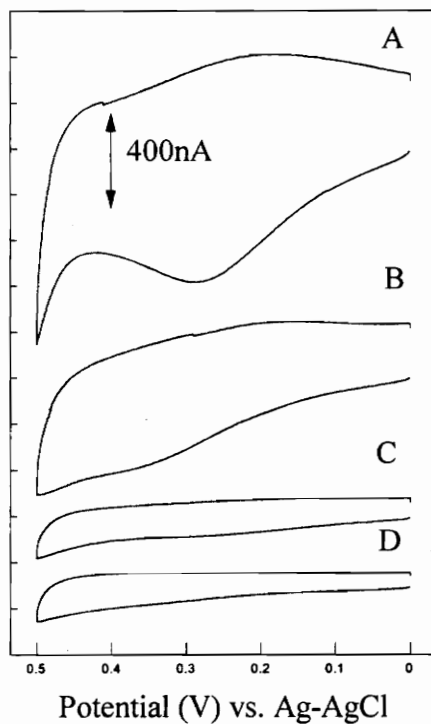


Figure 3.6. Cyclic voltammetry data in the presence of the acid containing dialkyl sulfide modified electrodes for aqueous 0.10 M NaCl solutions. Voltammogram A corresponds to the data for the  $\text{CH}_3(\text{CH}_2)_{17}\text{S}(\text{CH}_2)_{15}\text{COOH}$  monolayer, B to the data for the  $\text{CH}_3(\text{CH}_2)_{17}\text{S}(\text{CH}_2)_{10}\text{COOH}$  monolayer, C to the data for  $\text{CH}_3(\text{CH}_2)_{17}\text{S}(\text{CH}_2)_7\text{COOH}$ , and D to the data for an octadecanethiol monolayer for comparison. Other experimental conditions are given in Figure 3.5.

the octadecanethiol monolayer, suggesting an impenetrable structure for the aqueous solution. Our explanation is that for the  $\text{CH}_3(\text{CH}_2)_{17}\text{S}(\text{CH}_2)_7\text{COOH}$  monolayer, the pure hydrocarbon part of the molecule is much longer than the acid containing part (10 carbons longer), so it is possible for the  $-\text{COOH}$  group to be buried within the disordered methylene chains, preventing it from contacting the solution directly. This result correlates with the contact angle titration data for the  $\text{CH}_3(\text{CH}_2)_{17}\text{S}(\text{CH}_2)_7\text{COOH}$  monolayer.

Ellipsometry measurements on all the dialkyl sulfide modified surfaces were conducted, and the results are summarized in table 3.4. Ellipsometry shows that the physical dimensions of the three acid containing dialkyl sulfide monolayers are almost the same as each other (within the experimental error), and are only slightly smaller than that of an octadecanethiol monolayer. On the other hand, according to the charging current measurements, the relative thickness of the acid containing dialkyl sulfide monolayers decreases as the acid group is placed further from the substrate when in contact with aqueous solutions and under potential control. We believe that this dimensional difference is attributed to the penetration of aqueous solution through the acid containing dialkyl sulfide



Table 3.4. Thickness of the Unsymmetrical Dialkyl Sulfide Monolayers Measured by Optical Ellipsometry.

| Compounds  | thickness (angstrom) |
|--|----------------------|
| octadecanethiol  | $23 \pm 1$           |
| $\text{CH}_3(\text{CH}_2)_{17}\text{S}(\text{CH}_2)_{17}\text{CH}_3$ | $18 \pm 2$           |
| $\text{CH}_3(\text{CH}_2)_{17}\text{S}(\text{CH}_2)_9\text{CH}_3$    | $19 \pm 1$           |
| $\text{CH}_3(\text{CH}_2)_{17}\text{S}(\text{CH}_2)_7\text{CH}_3$    | $19 \pm 2$           |
| $\text{CH}_3(\text{CH}_2)_{17}\text{S}(\text{CH}_2)_{15}\text{COOH}$ | $16 \pm 5$           |
| $\text{CH}_3(\text{CH}_2)_{17}\text{S}(\text{CH}_2)_{10}\text{COOH}$ | $17 \pm 3$           |
| $\text{CH}_3(\text{CH}_2)_{17}\text{S}(\text{CH}_2)_7\text{COOH}$    | $18 \pm 4$           |

monolayers. Because of the presence of the polar carboxylic acid group, the monolayer is able to interact with an adjacent aqueous solution. A local polar region in the monolayer may be solvated by the surrounding water. The aqueous electrolyte solution is thus induced into the monolayer when a potential is applied. It is clear that the polar acid group plays a very important role in determining the permeability of the monolayer for aqueous solution. As an interesting comparison, the purely hydrocarbon dialkyl sulfide monolayers do not have a functional group that can interact with adjacent aqueous solution; consequently, purely hydrocarbon dialkyl sulfide monolayers are unable to allow aqueous solution to penetrate even though the monolayer has a disordered structure.

### 3.3.2 Cyclic Voltammetry

Cyclic voltammetry for the oxidation of an aqueous  $0.004 \text{ M Fe(CN)}_6^{4-}$  at the dialkyl sulfide modified electrodes was conducted in order to confirm our previous findings. Figure 3.7 shows the results of purely hydrocarbon dialkyl sulfide monolayers. Similar to the charging current data, there is little difference in the observed faradaic current between the three different hydrocarbon dialkyl sulfides, and the current is approximately the same as what is observed for an octadecanethiol modified interface. This indicates that purely hydrocarbon dialkyl sulfide monolayers can block the faradaic process effectively, even if they have disordered surface structure. Figure 3.8 shows the cyclic voltammetry for the same aqueous  $\text{Fe(CN)}_6^{4-}$  solution at the acid containing dialkyl sulfide modified electrodes. Again, the

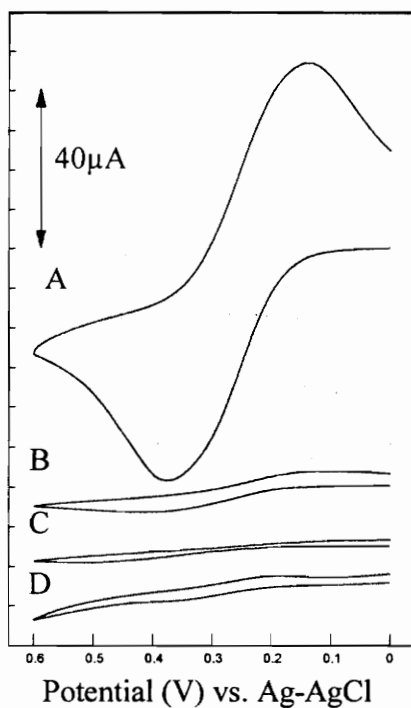


Figure 3.7. Cyclic voltammetry data for the oxidation of 0.004 M  $\text{Fe}(\text{CN})_6^{4-}$  in the presence of aqueous 0.10 M KCl at the hydrocarbon dialkyl sulfide modified electrodes. Voltammogram A corresponds to the response at an unmodified gold electrode, B to the data for the  $\text{CH}_3(\text{CH}_2)_{17}\text{S}(\text{CH}_2)_{17}\text{CH}_3$  monolayer, C to the data for  $\text{CH}_3(\text{CH}_2)_{17}\text{S}(\text{CH}_2)_9\text{CH}_3$  monolayer, and D to the data for the  $\text{CH}_3(\text{CH}_2)_{17}\text{S}(\text{CH}_2)_7\text{CH}_3$  monolayer. Other experimental conditions are given in figure 3.5.

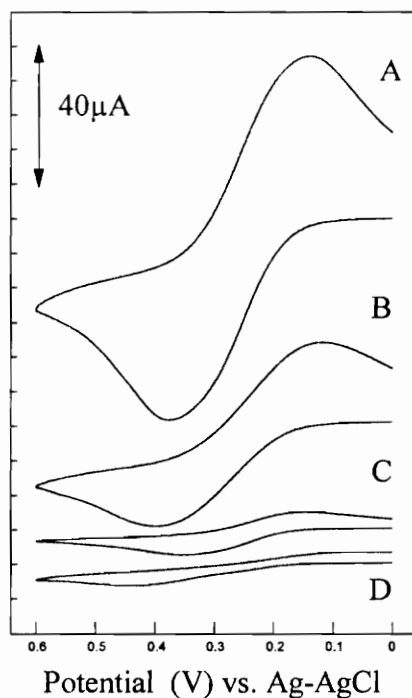


Figure 3.8. Voltammetry data for the oxidation of  $0.004\text{M Fe(CN)}_6^{4-}$  in the presence of aqueous  $0.10\text{ M KCl}$  at the acid containing dialkyl sulfide modified electrodes. Voltammogram A corresponds to the response at an unmodified gold electrode, B to the data for the  $\text{CH}_3(\text{CH}_2)_{17}\text{S}(\text{CH}_2)_{15}\text{COOH}$  monolayer, C to the data for  $\text{CH}_3(\text{CH}_2)_{17}\text{S}(\text{CH}_2)_{10}\text{COOH}$  monolayer, and D to the data for the  $\text{CH}_3(\text{CH}_2)_{17}\text{S}(\text{CH}_2)_{7}\text{COOH}$  monolayer. Other experimental conditions are given in figure 3.5.

amount of faradaic current is related to the proximity of the acid group to the interface. As the acid group is placed closer to the monolayer-solution interface, the amount of faradaic current observed increases. The increasing faradaic current observed as the acid group is placed closer to the interface indicates that the aqueous  $\text{Fe}(\text{CN})_6^{4-}$  has greater permeation into the monolayer, possibly due to the greater monolayer polarity experienced by the contacting solution. Consistent with our previous experimental results, for the  $\text{CH}_3(\text{CH}_2)_{17}\text{S}(\text{CH}_2)_7\text{COOH}$  monolayer, the faradaic current is the lowest of all three acid containing dialkyl sulfide monolayers, and is almost the same as that measured at the purely hydrocarbon dialkyl sulfide surfaces. The result again indicates that, for the  $\text{CH}_3(\text{CH}_2)_{17}\text{S}(\text{CH}_2)_7\text{COOH}$  monolayer, the acid group is efficiently protected by the hydrocarbon part of the molecule and isolated from the interfacial surface, making the monolayer hydrophobic in nature.

In summary, the ability of the solvent to interact with the monolayer structure is apparently the most important factor to determine the permeability and the charge transfer property of the SAM modified surface. For the two groups of dialkyl sulfide modified surfaces, although both of them demonstrated somewhat disordered surface structures, they have significantly different behaviors when in contact with aqueous solutions. This difference is due to the existence of the polar acid groups in the acid containing dialkyl sulfide modified surfaces. The acid group, when positioned near the monolayer-solution interface, can greatly increase the permeability and the charge transfer property of the SAM modified surface.

## Chapter 4

### Investigation of Terminal Functional Group Effects on Monolayers Prepared from $\omega$ -Mercaptoalkanoic Acids

From the first part of our research project, we found that the influence of polar groups within the monolayer structure played an important role in enhancing the charge transfer properties of the monolayer modified electrode, while disorder within the monolayer structure by itself was not enough to increase either the permeability or the charge transport properties of the electrode. We were particularly interested in the carbonyl region of the *ex situ* IR spectra of acid containing dialkyl sulfides (figure 3.2). As the carboxylic acid group is placed further from the sulfur atom of the dialkyl sulfide, the intensity of the carbonyl absorption decreases and nearly disappears into the noise for the monolayer prepared with  $\text{CH}_3(\text{CH}_2)_{17}\text{S}(\text{CH}_2)_{15}\text{COOH}$ . This observation suggested that the orientation of the acid group changes as a function of placement with the monolayer. The carbonyl absorption, when observed, is found at approximately  $1705\text{ cm}^{-1}$ , suggesting that the carboxylic acid groups are involved in hydrogen bonding interactions within the monolayer [22, 35].

The second part of the research project investigated how the interaction between carboxylic groups affect their alignments at the interface and how such alignments affect the permeabilities and/or charge transport properties of the monolayer modified electrode. In this part of the project, monolayers prepared from 15-mercaptopentadecanoic acid, 16-mercaptohexadecanoic acid, and their corresponding ethyl esters, were

studied. Again, the structure and the permeability of these monolayers were characterized by FTIR, contact angle measurements, and electrochemistry.

## 4.1 Infrared Spectroscopy

### 4.1.1 Comparison of IR Spectra in C-H region

*Ex situ* reflection infrared spectra for monolayers prepared from 15-mercaptopentadecanoic acid, 16-mercaptohexadecanoic acid, and their corresponding ethyl esters are shown in figure 4.1. Tetradecanethiol monolayers were used as a standard reference of an ordered, hydrocarbon monolayer. The important peaks are summarized in table 4.1. By comparison, the methylene modes of the carboxylic acid monolayers are positioned at higher energy than the corresponding modes for the ethyl ester and the tetradecanethiol monolayers (table 4.1). This result is thought to represent that the  $\omega$ -mercaptoalkanoic acid monolayers have a more fluid-like, disordered structure than the corresponding ethyl esters. The peak widths of the methylene modes of the  $\omega$ -mercaptoalkanoic acid monolayers also suggests a disordered structure (table 4.1): The peak widths of the carboxylic acid monolayers are much broader than the values of the esters and the tetradecanethiol (nearly twice the value).

With the two  $\omega$ -mercaptoalkanoic acid monolayers themselves, some slight but important differences are found between their spectra. First of all, the peak shapes of the methylene absorption are clearly different. The methylene modes of the 15-mercaptopentadecanoic acid are symmetrically shaped, and are positioned at higher energies (2926 and 2855  $\text{cm}^{-1}$ ) than found for tetradecanethiol monolayers (2919 and 2850  $\text{cm}^{-1}$ ). This peak

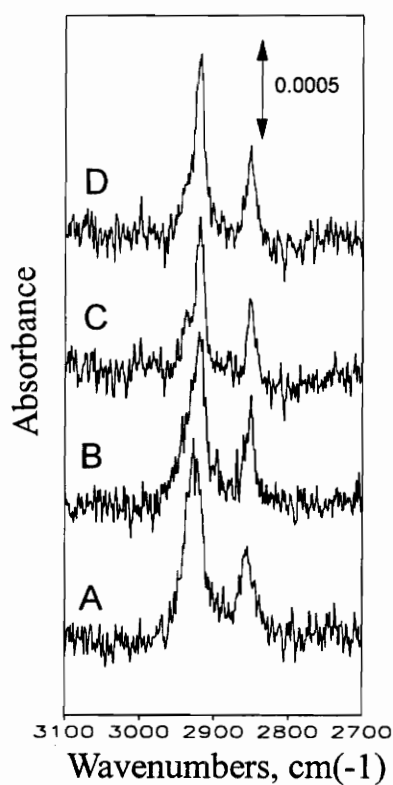


Figure 4.1. Reflection Infrared spectra of the C-H region for monolayers prepared from (A) 15-mercaptopentadecanoic acid, (B) 16-mercaptohexadecanoic acid, (C) the ethyl ester of 15-mercaptopentadecanoic acid, and (D) the ethyl ester of 16-mercaptohexadecanoic acid.



Table 4.1. Peak position and peak width (full width at half maximum) data for the reflection infrared spectra of monolayers prepared from tetradecanethiol, 15-mercaptopentadecanoic acid, 16-mercaptohexadecanoic acid, the ethyl ester of 15-mercaptopentadecanoic acid, and the ethyl ester of 16-mercaptohexadecanoic acid.

| Monolayer                                 | Asymmetric CH <sub>2</sub><br>(width) | Symmetric CH <sub>2</sub><br>(width) |
|---|---------------------------------------|--------------------------------------|
| Tetradecanethiol                          | 2919(13) cm <sup>-1</sup>             | 2850 (10) cm <sup>-1</sup>           |
| 15-mercaptopentadecanoic acid             | 2926 (29) cm <sup>-1</sup>            | 2855 (24) cm <sup>-1</sup>           |
| 16-mercaptohexadecanoic acid              | 2921 ( 29) cm <sup>-1</sup>           | 2851 (14) cm <sup>-1</sup>           |
| 15-mercaptopentadecanoic acid ethyl ester | 2918 (13) cm <sup>-1</sup>            | 2849 (12) cm <sup>-1</sup>           |
| 16-mercaptohexadecanoic acid ethyl ester  | 2919 (14) cm <sup>-1</sup>            | 2850 (16) cm <sup>-1</sup>           |

position is characteristic of a fluid structure for the 15-mercaptopentadecanoic acid monolayer. For the 16-mercaptohexadecanoic acid monolayer, the asymmetrical methylene absorption is unsymmetrically shaped, with a shoulder to higher energy. The peak position of the asymmetric methylene mode for the 16-mercaptohexadecanoic acid monolayer is  $2920\text{ cm}^{-1}$ . This position is a bit higher than that of the typical well-defined, crystalline-like monolayer structure such as the tetradecanethiol monolayer, but it is not as high as is found for the 15-mercaptopentadecanoic acid monolayer. These observations point out that there exists structural differences between the two carboxylic acid monolayers, even though they only have one methylene difference in the molecules that make up the monolayer. The IR data suggest that there exists some ordering of the alkyl chains in the 16-mercaptohexadecanoic acid monolayer, while the 15-mercaptopentadecanoic acid monolayer is largely disordered.

Many other researchers have also reported similar results with regard to the lower structural order observed with the  $\omega$ -mercaptoalkanoic acid monolayers [21, 35, 38]. For example, Chidsey and Loiacono found that the 11-mercaptoundecanoic acid monolayers had lower order than the corresponding alkyl mercaptan monolayers. They attributed this result to the steric effect of the carboxylic acid terminal group. They claimed that the size of the  $-\text{COOH}$  group prevented efficient assembly of the alkyl chains during the adsorption. Although this steric effect is a reasonable interpretation for carboxylic acid containing monolayers, it can not be applied to the spectral results of our ester monolayers. The ester

monolayers (table 4.1) are found to have very similar methylene peak position and width with those for the tetradecanethiol monolayer. In other words, even though there is a bulky carbonyl terminal group existing in ester monolayers like the  $\omega$ -mercaptoalkanoic acid monolayers, the ester monolayer structures are apparently still well ordered. The ordered nature of the ester monolayer is further confirmed by the low energy region of the infrared spectra (figure 4.2). Methylene twisting and wagging modes are found in these spectra, suggesting an ordered structure. Our results correspond with the work by Nuzzo *et al.* [22]. They suggested that the methyl ester of 16-mercaptohexadecanoic acid monolayer had aligned methylene chains in an all trans conformation. Both the 15-mercaptopentadecanoic acid and 16-mercaptohexadecanoic acid monolayers lack the methylene twisting and wagging modes at low energy that are observed in the corresponding ester spectra. This again indicates that the  $\omega$ -mercaptoalkanoic acid monolayers are not as ordered as found with the ester spectra.

#### 4.1.2 Comparison of Carbonyl Stretch in IR Spectra

The differences between 15-mercaptopentadecanoic acid and 16-mercaptohexadecanoic acid monolayers are more obvious in the low energy region of the infrared spectra (figure 4.3). For the 15-mercaptopentadecanoic acid monolayer, we found a single absorption at  $1715\text{ cm}^{-1}$ , which is assigned to the carbonyl involved in hydrogen bonding interactions. For the 16-mercaptohexadecanoic acid monolayer, however, there exists two bands in the carbonyl region. These two bands are centered

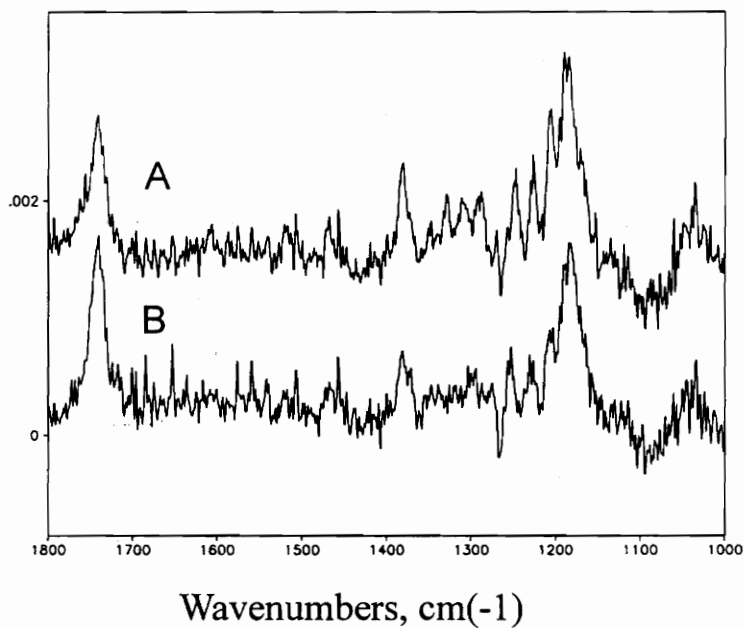


Figure 4.2. Reflection Infrared spectra of the low energy region of the spectrum for monolayers prepared from (A) the ethyl ester of 16-mercaptohexadecanoic acid, and (B) the ethyl ester of 15-mercaptopentadecanoic acid.

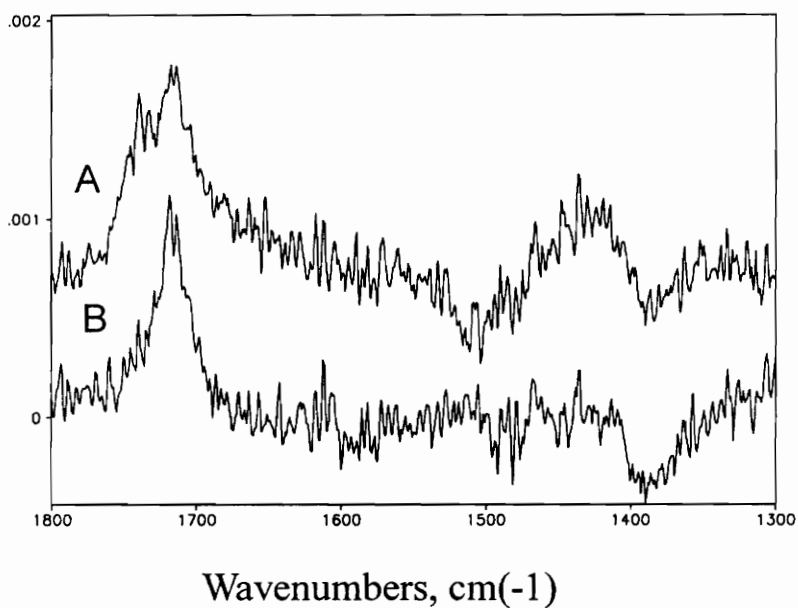


Figure 4.3. Reflection Infrared spectra of the low energy region of the spectrum for monolayers prepared from (A) 16-mercaptohexadecanoic acid, and (B) 15-mercaptopentadecanoic acid.

at  $1717\text{ cm}^{-1}$  and  $1740\text{ cm}^{-1}$ , and are assigned to an carbonyl stretch involved in hydrogen bonding and an carbonyl with weak or no hydrogen bonding, respectively [22, 35]. In other words, although 15-mercaptopentadecanoic acid and 16-mercaptohexadecanoic acid differ by only one methylene group, their low energy IR spectra indicate that they have significantly different interfacial structures, and this difference appears to be related to the extent of interaction ( i.e. hydrogen bonding ) among the functional groups.

The differences in the monolayer structures may be partially attributed to the so called even-odd effects that have been reported by other research groups [22, 23, 40]. For monolayers prepared from n-alkanethiols, the even or odd number of methylene groups in the alkyl chain, along with the overall tilt of the alkyl chain determine the projection of the terminal group with respect to the surface normal. According to the surface selection rule for reflection infrared spectroscopy, the projection of the terminal group should influence the intensity of the IR peak in the spectra. In our data, however, the spectra of 15-mercaptopentadecanoic acid and 16-mercaptohexadecanoic acid monolayers differ from each other not only by the absorption intensity, but also by the types of carbonyl modes observed. We believe that an even-odd effect explanation is only partially correct here. We suggest that another reason should be taken into account, namely, that the projection of the carboxylic acid group also influences the ability for carboxylic acid groups to interact with nearest neighbors. As a result, monolayers prepared from 15-mercaptopentadecanoic acid and 16-

mercaptohexadecanoic acid have different spectral features in the carbonyl region of the spectrum.

## 4.2 Contact Angle Measurements

Contact angle measurements on both carboxylic acid monolayers and ester monolayers were conducted. The results show that the contact angle values are different between the  $\omega$ -mercaptoalkanoic acid monolayers and the ester monolayers. The ester monolayers have a contact angle of  $80 \pm 2^\circ$ . This value is consistent with values found by Bain and co-workers [30], but are somewhat less than that for the tetradecanethiol monolayer ( $97 \pm 2^\circ$ ). This result indicates that the monolayers prepared from the ester molecules are less hydrophobic than the hydrocarbon surfaces. This may be attributed to the presence of the polar ester oxygens that can lower the interfacial contact angle.

For the carboxylic acid monolayers, the contact angle is lower than that of the ester monolayers, as expected because of the exposed carboxylic acid group at the interface. Again, however, a significant discrepancy between the 15-mercaptopentadecanoic acid and the 16-mercaptohexadecanoic acid monolayers is found. The contact angle of the 15-mercaptopentadecanoic acid monolayer is 35 degrees higher than that of the 16-mercaptohexadecanoic acid monolayer. The high contact angle value of 15-mercaptopentadecanoic acid monolayer suggests that a significant amount of hydrophobic methylenes are exposed at the interface. On the other hand, the lower contact angle value of 16-mercaptohexadecanoic acid monolayer suggests that fewer methylenes are

exposed to the surface, because the alkyl chains in 16-mercaptohexadecanoic acid monolayer are more ordered in nature. This conclusion is consistent with the previous IR measurements, where it is found that the peak position of the asymmetric methylene mode for the 16-mercaptohexadecanoic acid monolayer is lower than that for the 15-mercaptopentadecanoic acid monolayer, also suggesting a more ordered monolayer structure for the 16-mercaptohexadecanoic acid.

### **4.3 Electrochemistry: Charging Current Measurements**

Charging current measurements on both electrodes modified by carboxylic acid monolayers and ester monolayers were also conducted. The experiments were conducted by cyclic voltammetry on aqueous 0.10 M KCl solutions (figure 4.4, figure 4.5). Again, as a comparison, the charging current for tetradecanethiol modified electrode was also measured. For the two ester modified electrodes (figure 4.4), it is evident that the measured charging currents are similar to each other, and only slightly larger than that of the tetradecanethiol modified surface. This result is consistent with our previous IR measurements and contact angle measurements. It further confirms that the ester modified surfaces are only slightly more permeable to aqueous solution than a well ordered alkanethiol modified surface, despite the presence of a polar functional group. For the carboxylic acid monolayer modified electrodes (figure 4.5), it is obvious that their charging current is substantially larger than that of the corresponding esters. This result is also consistent with previous IR and contact angle measurements, where a lower structural order was suggested for these acid modified



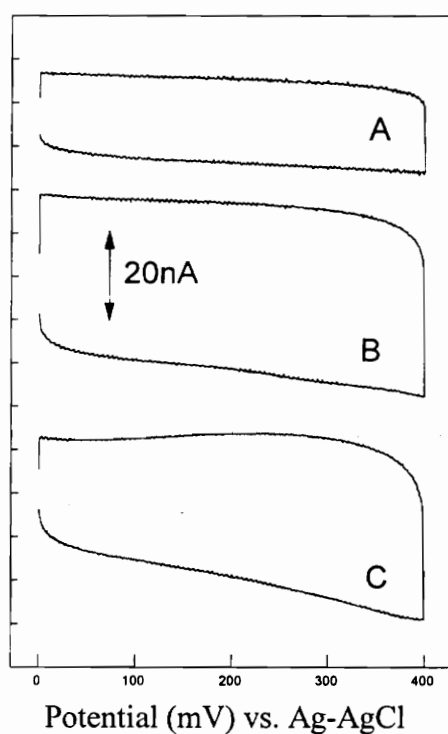


Figure 4.4. Current vs. Potential response to 0.10 M aqueous KCl at 100mV/sec for gold electrodes modified with (A) tetradecanethiol, (B) the ethyl ester of 15-mercaptopentadecanoic acid, and (C) the ethyl ester of 16-mercaptohexadecanoic acid.

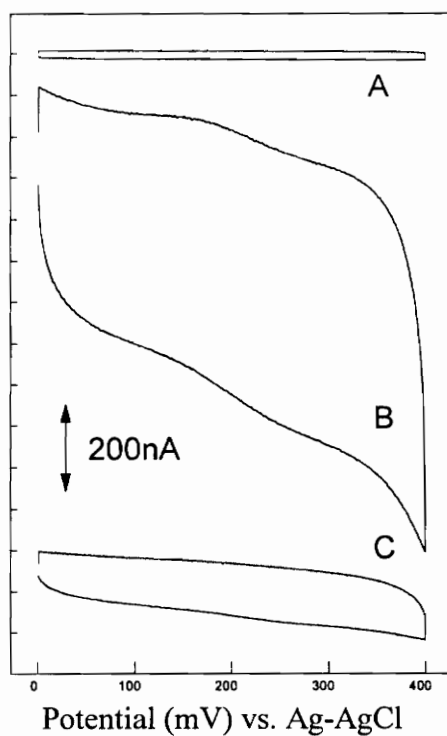


Figure 4.5. Current vs. Potential response to 0.10 M aqueous KCl at 100mV/sec for gold electrodes modified with (A) tetradecanethiol, (B) 15-mercaptopentadecanoic acid, and (C) 16-mercaptohexadecanoic acid.

surfaces. Here, we also notice that there exists a difference in the charging current between the two acid modified electrodes. The 15-mercaptopentadecanoic acid modified electrode has larger charging current than the 16-mercaptohexadecanoic acid modified electrode. This result again points to our previous conclusion that the 15-mercaptopentadecanoic acid monolayer has a more disordered structure than the 16-mercaptohexadecanoic acid monolayer, despite the fact that they only differ from one methylene group in molecule.

#### **4.4 Discussion and Conclusion**

Our previous experiments show that the measured data are strongly consistent with each other, all suggesting that the interfacial structure and properties are related to the intermolecular interactions (e.g., hydrogen bonding) among the terminal carboxylic acid groups. Other research groups also show that the interfacial structure and properties could be greatly influenced by interactions among terminal group within the monolayer [19, 20, 21, 41]. In our research, the two acid monolayers have the potential to be involved in hydrogen bonding, while the two ester monolayers can not. The formation of hydrogen bonds within the monolayer will evidently influence the interfacial structure and physical properties of the carboxylic acid monolayers. The differences in physical properties between the acid and the ester monolayers are, therefore, attributed to the structural disruption caused by a strong intermolecular interaction. The observation that the ester monolayers have similar physical properties to the tetradecanethiol monolayer, we believe that steric effects by themselves are

not powerful enough to largely influence the monolayer structure. Strong intermolecular interaction, such as hydrogen bonding, can have a much larger influence on the monolayer structure and its physical properties.

The differences between the 15-mercaptopentadecanoic acid monolayer and the 16-mercaptohexadecanoic acid monolayer are interesting since these monolayers only differ by one methylene group. It appears that such structural and physical differences are closely related with the extent of hydrogen bonding between the terminal carboxylic acid groups. According to IR measurements, the 15-mercaptopentadecanoic acid monolayers are extensively hydrogen-bonded, and they also have a more disordered monolayer structure. For the 16-mercaptohexadecanoic acid monolayers, there exists a significant amount of non-hydrogen bonding carbonyls, and these monolayers demonstrate a greater degree of order. As mentioned previously, the even-odd effect may contribute to the differences between the two carboxylic acid monolayers; however, the even-odd effect by itself cannot explain all of the experiment observations.

The driving force for the monolayer organization is the Van der Waals interactions between the methylene groups of adjacent alkyl chains. Our IR measurements with the 15-mercaptopentadecanoic acid monolayer suggest that extensive hydrogen bonding is present within the monolayer interface. The strong hydrogen bonding is apparently disruptive to the monolayer structure, possibly preventing Van der Waals interactions between adjacent methylene chains from driving the carbon chains to align on the surface. On the other hand, IR measurements show that 16-mercaptohexadecanoic acid monolayer does not have such extensive

hydrogen bonding. Compared with 15-mercaptopentadecanoic acid monolayer, 16-mercaptohexadecanoic acid monolayer is likely to be more stabilized by Van der Waals interactions because of the smaller extent of hydrogen bonding between the carboxylic acid groups.

In summary, the additional methylene group of the 16-mercaptohexadecanoic acid influences the projection of the acid group at the monolayer surface relative to that for the 15-mercaptopentadecanoic acid monolayer. The microscopic environment at the interface of the two acid monolayers is thus significantly different from each other. Consequently, the abilities to form hydrogen bonding among nearest neighbors are different for the two acid monolayers, and this difference can substantially influence the structural organization and physical properties of the monolayer.

## Chapter 5 Summary

In the first part of our project, the monolayer structure of two groups of dialkyl sulfides and their charge transport properties were characterized. We studied the influence of polar acid groups within the monolayer, as well as the importance of monolayer structural disorder upon the interfacial behavior (charge transport properties or permeabilities) of the SAM modified surface. It is found that the existence of disorder within the monolayer itself is not enough to enhance the charge transport properties and/or permeabilities to aqueous solution for the SAM surface. By introducing a polar carboxylic acid group into the monolayer, however, a significant increase in the charge transport properties and/or permeabilities is observed. The polar acid group is considered to be playing a very important role in determining the interfacial physical properties of the monolayer interface. The positioning of the polar acid group with respect to the surface is also critical. The charge transport properties and permeabilities are more enhanced when the polar acid group is placed closer to the monolayer-solution interface.

As a natural continuation of the first part of the project, we also studied monolayers prepared from  $\omega$ -mercaptoalkanoic acids and their corresponding esters. Different structural organizations and physical properties were found between the acids and esters. More interestingly, there also exists significant differences between monolayers prepared from 15-mercaptopentadecanoic acid and 16-mercaptohexadecanoic acid. We attribute these differences to the combined influence of the different spatial

projections of the terminal groups, and the projections consequent influence upon the abilities of the acid groups to form hydrogen bonds at the monolayer interface. The additional methylene group in 16-mercaptohexadecanoic acid monolayer apparently influences the spatial orientation of the acid carbonyl at the monolayer interface relative to that for the 15-mercaptopentadecanoic acid monolayer. This difference, we believe, dramatically influences the tendency to form hydrogen bonds for the two acid monolayers. Consequently, the surface structure and physical properties are significantly different for the two acid monolayers.

Our research project demonstrates that the interfacial properties of the SAM modified surface are greatly influenced by its structure and/or its composition. With a polar group embedded close to the monolayer-solution interface, the permeabilities or charge transfer properties of the SAM modified surface can be greatly enhanced. Hydrogen bonding or other intermolecular interactions, if they exist, may also largely influence the interfacial properties of the SAM modified surface. However, such interactions are sensitive to the projection and/or intermolecular distance. Our research demonstrates that the surface structure of monolayers and its interfacial properties are complicated phenomena. Many different factors contribute to the overall behavior of the SAM modified surface. Using sophisticated surface-bound species to modify surface is proven to be an effective method to investigate how different structural properties influence interfacial behavior.

## References

1. R.G. Nuzzo, and D.L. Allara, *J. Am. Chem. Soc.* **1983**, 105, 4481.
2. Swalen, J. D.; Allara, D. L.; Andrade, J. D.; Chandross, E. A.; Garoff, S.; Isrealachvili, J.; McCarthy, T. J.; Murry, R.; Pease, R. F.; Rabolt, J. F.; Wynne, K. J.; Yu, H. *Langmuir* **1987**, 3, 932.
3. Bain, C. D.; Whitesides, G. M. *J. Am. Chem. Soc.* **1992**, 114, 1990-1995.
4. Bain, C. D.; Whitesides, G. M. *Langmuir* **1989**, 5, 1370-1378.
5. Chidsey, C. E. D.; Bertozzi, C. R.; Putvinski, T. M.; Mujsce, A. M. *J. Am. Chem. Soc.* **1990**, 112, 4301-4306.
6. Pale-Grosdemange, C.; Simon, E. S.; Prime, K. L.; Whitesides, G. M. *J. Am. Chem. Soc.* **1991**, 113, 12-20.
7. Evans, S. D.; Gopper-Berarducci, K. E.; Urankar, E.; Gerenser, L. J.; Ulman, A.; Snyder, R. G. *Langmuir* **1991**, 7, 2700-2709.
8. Troughton, E. B.; Bain, C. D.; Whitesides, G. M.; Nuzzo, R. G.; Allara, M. D. *Langmuir* **1988**, 4, 365.
9. Sagiv, J. *J. Am. Chem. Soc.* **1980**, 102, 92.
10. Bilewicz, R.; Majda, M. *J. Am. Chem. Soc.* **1991**, 113, 5464.
11. Sabatani, E.; Rubinstein, I. *J. Phys. Chem.* **1987**, 91, 6663.
12. Chailapakul, O.; Crooks, R. M. *Langmuir* **1993**, 9, 884-888.
13. Finklea, H. O.; Avery, S.; Lynch, M.; Furtsch, R. *Langmuir* **1987**, 3, 409.
14. Wang, J.; Hui, w.; Angnes, L. *Anal. Chem.* **1993**, 65, 1893.



15. Takehara, K. O.; Takenura, H.; Ide, I. *J. Colloid Interface Sci.* **1993**, 156, 274.
16. Sandroff, C. J.; Garoff, S.; Leung, K. P. *Chem. Phys. Lett.* **1983**, 96, 547.
17. Stole, S. M.; Porter, M. D. *Langmuir* **1990**, 6, 1192.
18. Anderson, M. R.; Gatin, M. R. *Langmuir* **1994**, 10, 1638.
19. Miller, C.; Cuendet, P.; Gratzel, M. *J. Phys. Chem.* **1991**, 95, 877.
20. Miller, C.; Gratzel, M. *J. Phys. Chem.* **1991**, 95, 5225.
21. Chidsey, C. E. D.; Loiacano, D. N. *Langmuir* **1990**, 6, 682.
22. Nuzzo, R. G.; Dubois, L. H.; Allara, D. L.; *J. Am. Chem. Soc.* **1990**, 112, 558.
23. Tao, Y. T. *J. Am. Chem. Soc.* **1993**, 115, 4350.
24. Widrig, C. A.; Chung, C.; Proter, M. D. *J. Electroanal. Chem.* **1991**, 310, 335.
25. Stole, S. M.; Porter, M. D. *Langmuir* **1990**, 6, 1199.
26. Allara, D. L.; Nuzzo, R. G. *Langmuir* **1985**, 1, 52.
27. Pearce, H. A.; Sheppard, N. *Surface Sci.* **1976**, 59, 205.
28. Adamson, A. W. *Physical Chemistry of Surfaces*, 4th Ed., Wiley, New York (1982).
29. Porter, M. D.; Bright, T. B.; Allara, D. L.; Chidsey, C. E. D. *J. Am. Chem. Soc.* **1987**, 109, 3559.
30. Bain, D. D.; Troughton, E. B.; Tao, Y. T.; Evall, J.; Whitesides, G. M.; Nuzzo, R. G. *J. Am. Chem. Soc.* **1989**, 111, 321.

31. Dobbs, D. A.; Bergman, R. G.; Theopold, K. H. *Chem. Eng. News* **1990**, 68(17), 2.
32. Hill, I. R.; Levin, I. W. *J. Chem. Phys.* **1979**, 70, 842.
33. Bain, C. D.; Whitesides, G. M. *J. Am. Chem. Soc.* **1988**, 110, 3664.
34. Bain, C. D.; Whitesides, G. M. *J. Am. Chem. Soc.* **1989**, 111, 7164.
35. Duevel, R. V.; Corn, R. M. *Anal. Chem.* **1992**, 64, 337.
36. Whitesides, G. M.; Laibinis, P. E. *Langmuir* **1990**, 6, 87.
37. Smith, E. L.; Alves, C. A.; Anderegg, J. W.; Porter, M. D.; Siperko, L. M. *Langmuir* **1992**, 8, 2707.
38. Sun, L.; Crooks, R. M.; Ricco, A. J. *Langmuir* **1993**, 9, 1775.
39. Groat, K. A.; Creager, S. E. *Langmuir* **1993**, 9, 3668.
40. Laibinis, P. E.; Whitesides, G. M.; Allara, D. L.; Tao, Y. T.; Parikh, A. N.; Nuzzo, R. G. *J. Am. Chem. Soc.* **1991**, 113, 7152.
41. Sellers, H.; Ulman, A.; Shnidman, Y.; Eilers, J. E. *J. Am. Chem. Soc.* **1993**, 115, 9389.
42. Bard, A. J.; Faulkner, L. R. *Electroanalytical Methods*, Wiley, New York, **1980**.

## Vita

Minhui Zhang was born in Jiangsu Province, P.R. China, on October 7, 1966. Upon graduation from high school in 1988, Minhui went to Fudan University in Shanghai, China as a Chemistry major. He graduated with a Bachelor's degree in Analytical Chemistry and was hired by Meishan Metallurgical Company in Nanjing, China as a Chemical Engineer. In 1993, he came to Virginia Polytechnic Institute and State University to pursue his graduate degree. His research advisor is Professor Mark R. Anderson.

Minhui married Meiding Zhang in 1990. Their son, Oliver Zhang, was born on July 8, 1991.

### Publications

1. Minhui Zhang and M. R. Anderson, "Investigation of the Charge Transfer Properties of Electrodes Modified by the Spontaneous Adsorption of Unsymmetrical Dialkyl Sulfides", *Langmuir*, 1994, 10, 2807.

2. M. R. Anderson, M. Evaniak, Minhui Zhang, "Application of Polarization Modulation Infrared Reflection Adsorption Spectroscopy to study the *In situ* Structure of Monolayers Prepared by Spontaneous Adsorption", *Langmuir*, 1996, 12, 2327.

3. M. R. Anderson, Minhui Zhang, and Joon Lee, "Observation of Even-odd effects with Monolayers Prepared from  $\omega$ -Mercaptoalkanoic Acids", submitted.

